Tamura K and Ohashi Y. (2003). *Int. J. Hematol.*, **77**, 512–517.
Toyota M, Ho C, Ahuja N, Jair KW, Li Q, Ohe-Toyota M, Baylin SB and Issa JP. (1999). *Cancer Res.*, **59**, 2307–2312.
Tsuda H, Takatsuki K, Ohno R, Masaoka T, Okada K, Shirakawa S, Ohashi Y and Ota K. (1994). *Br. J. Cancer*, **70**, 771–774.
Tsukasaki K, Ikeda S, Murata K, Maeda T, Atogami S, Sohda H, Momita S, Jubashi T, Yamada Y, Mine M, Kamihira S and Tomonaga M. (1993). *Leuk. Res.*, **17**, 157–166.
Tsukasaki K, Tobinai K, Shimoyama M, Kozuru M, Uike N, Yamada Y, Tomonaga M, Araki K, Kasai M, Takatsuki K, Tara M, Mikuni C and Hotta T. (2003). *Int. J. Hematol.*, **77**, 164–170.
Uike N, Choi I, Tokoro A, Goto T, Yufu Y, Kozuru M and Tobinai K. (1998). *Intern. Med.*, **37**, 411–413.
Uozumi K, Hanada S, Ohno N, Ishitsuka K, Shimotakahara S, Otsuka M, Chyuman Y, Nakahara K, Takeshita T, Kuwazuru Y, Saito T, Makino T, Iwahashi M, Utsunomiya A and Arima T. (1995). *Leuk. Lymphoma*, **18**, 317–323.
Utsunomiya A, Miyazaki Y, Takatsuka Y, Hanada S, Uozumi K, Yashiki S, Tara M, Kawano F, Saburi Y, Kikuchi H, Hara M, Sao H, Morishima Y, Kodera Y, Sonoda S and Tomonaga M. (2001). *Bone Marrow Transplant*, **27**, 15–20.
Waldmann TA, Goldman CK, Bongiovanni KF, Sharrow SO, Davey MP, Cease KB, Greenberg SJ and Longo DL. (1988). *Blood*, **72**, 1805–1816.
Waldmann TA, White JD, Carrasquillo JA, Reynolds JC, Paik CH, Gansow OA, Brechbiel MW, Jaffe ES, Fleisher TA, Goldman CK, Top LE, Bamford R, Zaknoen E, Roessler E, Kasten-Sportes C, England R, Litou H, Johnson JA, Jackson-White T, Manns A, Hanchard B, Junghans RP and Nelson DL. (1995). *Blood*, **86**, 4063–4075.
Waldmann TA, White JD, Goldman CK, Top L, Grant A, Bamford R, Roessler E, Horak ID, Zaknoen S, Kasten-Sportes C, England R, Horak E, Mishra B, Dipre M, Hale P, Fleisher TA, Junghans RP, Jaffe ES and Nelson DL. (1993). *Blood*, **82**, 1701–1712.
Watanabe T, Yamaguchi K, Takatsuki K, Osame M and Yoshida M. (1990). *J. Exp. Med.*, **172**, 759–765.
Welles SL, Tachibana N, Okayama A, Shioiri S, Ishihara S, Murai K and Mueller NE. (1994). *Int. J. Cancer*, **56**, 337–340.
Wu X, Li Y, Crise B and Burgess SM. (2003). *Science*, **300**, 1749–1751.
Yamada Y, Hatta Y, Murata K, Sugawara K, Ikeda S, Mine M, Maeda T, Hirakata Y, Kamihira S, Tsukasaki K, Ogawa S, Hirai H, Koeffler HP and Tomonaga M. (1997). *J. Clin. Oncol.*, **15**, 1778–1785.
Yamada Y and Tomonaga M. (2003). *Leuk. Lymphoma*, **44**, 611–618.
Yamada Y, Tomonaga M, Fukuda H, Hanada S, Utsunomiya A, Tara M, Sano M, Ikeda S, Takatsuki K, Kozuru M, Araki K, Kawano F, Niimi M, Tobinai K, Hotta T and Shimoyama M. (2001). *Br. J. Haematol.*, **113**, 375–382.
Yasunaga J, Sakai T, Nosaka K, Etoh K, Tamiya S, Koga S, Mita S, Uchino M, Mitsuya H and Matsuoka M. (2001). *Blood*, **97**, 3177–3183.
Yasunaga J, Taniguchi Y, Nosaka K, Yoshida M, Satou Y, Sakai T, Mitsuya H and Matsuoka M. (2004). *Cancer Res.*, **64**, 6002–6009.
Yoshida M. (2001). *Annu. Rev. Immunol.*, **19**, 475–496.
Yoshida M, Nosaka K, Yasunaga J, Nishikata I, Morishita K and Matsuoka M. (2004). *Blood*, **103**, 2753–2760.
Zhang Z, Zhang M, Goldman CK, Ravetch JV and Waldmann TA. (2003). *Cancer Res.*, **63**, 6453–6457.

[CANCER RESEARCH 64, 6002–6009, September 1, 2004]

Identification of Aberrantly Methylated Genes in Association with Adult T-Cell Leukemia

Jun-ichirou Yasunaga,[1] Yuko Taniguchi,[1] Kisato Nosaka,[1] Mika Yoshida,[1] Yorifumi Satou,[1] Tatsunori Sakai,[2] Hiroaki Mitsuya,[2] and Masao Matsuoka[1]

[1]Laboratory of Virus Immunology, Institute for Virus Research, Kyoto University, Kyoto, Japan; and [2]Department of Internal Medicine II, Kumamoto University School of Medicine, Kumamoto, Japan

ABSTRACT

In this study, we identified 53 aberrantly hypermethylated DNA sequences in adult T-cell leukemia (ATL) cells using methylated CpG island amplification/representational difference analysis method. We also observed a proportionate increase in the methylation density of these regions with disease progression. Seven genes, which were expressed in normal T cells, but suppressed in ATL cells, were identified near the hypermethylated regions. Among these silenced genes, *Kruppel-like factor 4* (*KLF4*) gene is a cell cycle regulator and *early growth response 3* (*EGR3*) gene is a critical transcriptional factor for induction of Fas ligand (FasL) expression. Treatment with 5-aza-2′-deoxycytidine resulted in the recovery of their transcription, indicating that their silencing might be associated with DNA hypermethylation. To study their functions in ATL cells, we transfected recombinant adenovirus vectors expressing *KLF4* and *EGR3* genes. Expression of *KLF4* induced apoptosis of ATL cells whereas enforced expression of *EGR3* induced the expression of *FasL* gene, resulting in apoptosis. Thus, suppressed expression of *EGR3* enabled ATL cells to escape from activation-induced cell death mediated by FasL. Our results showed that the methylated CpG island amplification/representational difference analysis method allowed the isolation of hypermethylated DNA regions specific to leukemic cells and thus shed light on the roles of DNA methylation in leukemogenesis.

INTRODUCTION

Human T-cell leukemia virus type I (HTLV-I) is the causative retrovirus of a neoplastic disease, adult T-cell leukemia (ATL) and an inflammatory disease, HTLV-I-associated myelopathy/tropical spastic paraparesis (1–4). After infection with HTLV-I, a small proportion of carriers (about 2–5%) develop ATL after a long latent period (5). In this virus-induced leukemia, viral proteins encoded by HTLV-I play an important role in the proliferation of infected cells and leukemogenesis. Among them, Tax is considered to play a central role in leukemogenesis because of its pleiotropic actions (6, 7), such as transcriptional activation of cellular genes (8–10), *trans*-repression of cellular genes transcription (11, 12), and functional inactivation of p53 and MAD1 (12, 13). These pleiotropic functions render HTLV-I-infected cells able to proliferate, and confer resistance to apoptotic signals, resulting in clonal expansion.

In the late stage of leukemogenesis, *tax* is frequently inactivated through several mechanisms (14) such as loss of 5′-long terminal repeat (LTR) (15), genetic alterations of *tax* gene (16), and DNA hypermethylation in 5′-LTR (17), indicating that Tax is not always necessary for leukemogenesis. Because Tax is the major target molecule of CTLs *in vivo* (18), the expression of Tax confers a growth advantage to infected cells, but on the other hand, it renders infected cells susceptible to CTLs. Fully transformed ATL cells are considered to acquire the ability to proliferate *in vivo* in the absence of Tax expression. Such a transformation process is thought to include alterations of host genome: genetic and epigenetic changes. Although the genetic changes, such as mutation of *p53* (19) and deletion of *p16* (20, 21), in ATL cells were reported, they are not frequent and are observed predominantly in the late stage of the disease.

In addition to genetic alterations, DNA hypermethylation of promoter region CpG islands has been analyzed in the context of oncogenesis because this process silences gene transcription of tumor-suppressor genes. This epigenetic alteration is observed commonly in various cancer cells. Although methylation "profiling" studies have shown that some genes are frequently methylated in various tumor cells, other genes are methylated in a tumor-type-specific manner (22, 23). To date, several methods have been developed to isolate differentially methylated DNA regions in cancers (24–29). Recently, with methylated CpG island amplification/representational difference analysis (MCA/RDA) method, we isolated hypomethylated DNA regions and demonstrated that *MEL1S* gene was hypomethylated and aberrantly transcribed in ATL cells (30).

The present study was designed to isolate hypermethylated DNA regions in ATL cells compared with cells in the carrier state using the MCA/RDA method and to identify those genes that have an expression associated with DNA hypermethylation. On the basis of our results, we discuss the association between aberrant DNA methylation and leukemogenesis of ATL.

MATERIALS AND METHODS

Cells. Peripheral blood mononuclear cells (PBMCs) were isolated from 10 patients with ATL (five acute type cases and five chronic type cases), five asymptomatic carriers, and five uninfected individuals using Ficoll-Paque density centrifugation method. We also used the cell lines ED, ATL-43T, ATL-48T, ATL-55T, MT-1, and TL-Oml, which were derived from leukemic clones, and MT-2, which is derived from nonleukemic cells. To study the effect of demethylation, ATL-43T was cultured in media supplemented with 10 μmol/l 5-aza-2′-deoxycytidine (5-aza-dC; Sigma, St. Louis, MO) for 3 days, 10 μmol/l 5-aza-dC and 1 μmol/l trichostatin A (TSA; Sigma) for the last 24 hours, or 1 μmol/l TSA for 24 hours alone. The human embryonic kidney cell line, HEK 293, was used for the packaging of recombinant adenovirus vectors.

Viral FLICE-inhibitory protein (FLIP) derived from the equine herpes virus type 2, E8 (31), and the long form of murine cellular FLIP (mCasper$_L$; Ref. 32) expression vectors were transfected into ATL-43T cells by electroporation with a Gene Pulser II (Bio-Rad, Hercules, CA). Stable transfectants were selected and maintained in culture medium containing G418 (500 μg/ml; Nacalai tesque, Kyoto, Japan). The transfected cell lines by each of the vectors were designated as ATL-43T-E8 and ATL-43T-mCas, respectively.

Methylated CpG Island Amplification/Representational Difference Analysis. To identify aberrantly hypermethylated DNA regions in ATL cells, we used the MCA/RDA method, as reported previously (28). Five micrograms of genomic DNA were digested with 100 units of *Sma*I (New England Biolabs, Beverly, MA) twice and then digested once with 20 units of *Xma*I (New England Biolabs). RMCA adaptor was prepared by annealing of the oligonucleotides RMCA24 (5′-CCACCGCCATCCGAGCCTTTCTGC-3′) and

Received 4/26/04; revised 6/15/04; accepted 6/25/04.

Grant support: Grant-in-Aid for Scientific Research from the Ministry of Education, Science, Sports, and Culture of Japan.

The costs of publication of this article were defrayed in part by the payment of page charges. This article must therefore be hereby marked *advertisement* in accordance with 18 U.S.C. Section 1734 solely to indicate this fact.

Note: Supplementary data for this article can be found at Cancer Research Online (http://cancerres.aacrjournals.org).

Requests for reprints: Jun-ichirou Yasunaga, Laboratory of Virus Immunology, Institute of Virus Research, Kyoto University, Kyoto 606-8507, Japan. Phone: 81-75-751-4048; Fax: 81-75-751-4049; E-mail: jyasunag@virus.kyoto-u.ac.jp.

RMCA12 (5′-CCGGGCAGAAAG-3′), and ligated to the digested DNA fragments using T4 DNA ligase (New England Biolabs). To amplify the hypermethylated DNA fragments, which were ligated adaptors in both ends, PCR was performed using the RMCA24 oligonucleotides as primers. The amplicons were synthesized using samples from an ATL patient and a HTLV-I carrier. For detection of ATL cell-specific hypermethylated DNA sequences, MCA products from a carrier were used as a driver of RDA, and those products from an acute ATL patient as a tester. We used GeneFisher Basic Reagent Set (TaKaRa, Shiga, Japan) for RDA. In RDA step, 500 and 100 ng of ligation mixture were used for the first and second selective PCR, respectively. Oligonucleotides used for RDA were JMCA24 (5′-GTGAGGGTCGGATCTGGATGGCTC-3′), JMCA12 (5′CCGGGAGCCAGC-3′), NMCA24 (5′-GTTAGCGGACACAGGGCGGGTCAC-3′), and NMCA12 (5′-CCGGGTGACCCG-3′). Subcloning of the MCA/RDA products was carried out using pCR-XL-TOPO (Invitrogen, Carlsbad, CA) or pGEM-T Easy (Promega, Madison, WI) as vectors, and then the sequences of each fragment were determined by PCR using M13 primers. Sequence homologies and localization in chromosomes were identified using the BLAST program of the National Center for Biotechnology Information.[3]

MCA-Southern Hybridization. To confirm that the isolated DNA regions are specifically hypermethylated in ATL cells, Southern blot method was used. MCA products from an ATL patient and a HTLV-I carrier (500-ng each) were separated by electrophoresis in 1.5% agarose gels and then transferred to Hybond-N + (Amersham Biosciences, Piscataway, NJ). All of the isolated DNA fragments were labeled with ^{32}P, and hybridized to these filters.

Combined Bisulfite Restriction Analysis and Bisulfite Sequencing Analysis. For nine DNA regions identified by MCA/RDA, the methylation status of the DNA regions was determined by Combined Bisulfite Restriction Analysis or bisulfite sequencing as described previously (33). First, genomic DNAs were treated with sodium bisulfite (34) and then amplified by nested PCR using the specific primers listed in Supplementary Table 1. The PCR products of these regions were digested with *Taq*I (New England Biolabs) or *Acc*II (TaKaRa), subjected to electrophoresis in 3% agarose gels, and visualized by ethidium bromide staining. The percentage of DNA methylation was calculated by the intensities of methylation and unmethylation signal determined by ATTO densitometry software (ATTO, Tokyo, Japan).

For detailed analysis of DNA methylation in *Kruppel-like factor 4* (*KLF4*) and *early growth response 3* (*EGR3*) genes, we performed bisulfite sequencing. The PCR products of the isolated regions and promoter regions of these genes were subcloned into pGEM-T Easy, thereafter, the sequences of each of 10 clones were determined. Because the promoter sequence of *KLF4* has not been determined, we predicted its sequence using the program[4] supported by the BioInformatics & Molecular Analysis Section, Computational Bioscience and Engineering Lab, Center for Information Technology, and NIH. Primers for bisulfite sequencing are also listed in Supplementary Table 1.

Semi-quantitative Reverse Transcriptase-PCR. Total RNA was extracted from the PBMCs and cell lines using Trizol reagent (Invitrogen) and then treated DNaseI (Invitrogen). cDNAs were synthesized from 0.5 μg of total RNA with the Superscript First-Strand Synthesis System for reverse transcription (RT)-PCR (Invitrogen) and used for semi-quantitative RT-PCR as template. The primers used for RT-PCR and their annealing temperatures are summarized in Supplementary Table 2. The number of PCR cycles was appropriately determined for each quantification (Supplementary Table 2). We used 1.25 units of ExTaq polymerase (TaKaRa) for each reaction. All experiments were performed including samples of whole brain (Clontech, Palo Alto, CA) and skeletal muscle (Stratagene, La Jolla, CA) as positive control of PCR reaction.

Construction of Adenovirus Vectors. The recombinant adenovirus vectors containing *KLF4* and *EGR3* gene (KLF4-AD and EGR3-AD, respectively) were generated using Adeno-X Expression System (Clontech) according to the manufacturer's protocol. These adenovirus vectors were concentrated and purified by Virakit for adenovirus 5 and recombinant derivatives (Virapur, San Diego, CA), and then the viral titers were determined using Adeno-X Rapid Titer Kit (Clontech). The *lacZ*-containing adenovirus vector (lacZ-AD) was also prepared as a negative control. All adenovirus vectors were used to infect an ATL cell line, ATL-43T, at 1,000 infectious units/cell.

Flow Cytometric Analysis. The flow cytometry (model EPICS XL flow cytometer, Beckman Coulter, Miami Lakes, FL) was used for analyses of apoptosis. Annexin V-FITC/PI double staining and terminal-deoxynucleotidyl transferase-mediated dUTP-FITC nick-end labeling (TUNEL) assay were performed for detection of apoptosis, using MEBCYTO apoptosis kit (MBL, Nagoya, Japan) and MEBSTEIN apoptosis kit direct (MBL), respectively.

RESULTS

Isolation of Hypermethylated DNA Regions in the Genome from ATL Cells. To identify hypermethylated regions in the genome of ATL cells, we carried out MCA/RDA, which was used previously to isolate a number of methylated CpG islands in colon cancer cell line (28). MCA products were generated from the genomic DNA of a carrier (driver) and an acute ATL patient (tester). After the second round of RDA, the PCR products were subcloned, and their sequences were determined. To confirm that identified DNA fragments were amplified in tester amplicon, we examined whether isolated DNA fragment specifically hybridized to the tester amplicon using Southern blot method (MCA-Southern). Specific hybridization to the tester amplicon implied that isolated DNA regions were hypermethylated in ATL cells compared with peripheral blood mononuclear cell (PBMC) from a carrier. Finally, we identified 53 differentially hypermethylated DNA fragments in ATL cells. The chromosomal locations of all of the fragments were analyzed by NCBI BLAST program. We tested whether these identified regions satisfied the criteria for CpG islands proposed by Takai and Jones (35). The results revealed that the majority of clones (48 of 53 clones) were located in CpG islands. Information of isolated sequences is described in Table 1.

Accumulation of Aberrant DNA Hypermethylation during Disease Progression. Chronic ATL is characterized as an indolent form, which later progresses to aggressive forms (*i.e.*, acute or lymphoma-type ATL). To confirm that DNA hypermethylation identified in this study is associated with disease progression, we analyzed the extent of DNA methylation of nine DNA regions at different stages by Combined Bisulfite Restriction Analysis. Fig. 1*A* shows the profiles of the methylation status in these DNA fragments. In cell lines, CpG sites in identified DNA fragments were highly methylated, which was consistent with the finding of DNA methylation in the established cell lines. This confirmed that the isolated DNA regions were hypermethylated in ATL cells and that MCA-Southern could identify the hypermethylated DNA regions. In the carrier state, most DNA fragments were unmethylated. On the other hand, they were frequently methylated in chronic ATL, and the level of methylation increased in acute ATL, indicating that DNA methylation in the isolated DNA regions tends to accumulate according to disease progression. This was also confirmed in the sequential samples from a HTLV-I carrier, who developed acute ATL (Fig. 1*B*).

Identification of Genes near the Hypermethylated DNA Regions. To analyze the influence of identified DNA hypermethylation upon gene transcription, the neighboring genes were searched using NCBI BLAST program as described in Materials and Methods. We found that 31 of 53 (58%) clones were located within the exon or intron of the gene, and 41 of 53 (77%) loci were located within 10 kb from the transcriptional start site of the nearest gene (Table 1). Because the aberrant methylation of some identified genes, such as *PAX5* (clone 10; ref. 36) and *CSPG2* (clone 27; ref. 28), have been reported in various types of cancer cells, it confirmed that MCA/RDA method in this study isolated the hypermethylated DNA regions. Then, we analyzed the transcription of genes in which the transcriptional start sites existed within 2 kb from the identified hypermethylated DNA regions (Fig. 2). On the basis of their expression profiles, we could divide the genes identified into two groups; group I con-

[3] http://www.ncbi.nlm.nih.gov/BLAST/.
[4] http://bimas.dcrt.nih.gov:80/molbio/proscan/.

Table 1 *Characterization of DNA fragments isolated by MCA/RDA*

Clone	Size (bp)	Accession no. (location)	Chromosomal location	Nearest gene	CpG Island	Distance from TSS (bp)
1	733	NT_007592.13 (19499884–19500616)	6p21.31	*No gene**	Yes	
2	511	NT_006713.13 (6324465–6324975)	5q13.3	*OTP*	Yes	2,600
3	377	NT_025741.13 (5075242–5075619)	6q16.3	*SIM1*	Yes	5,800
4	486	NT_079617.1 (40630–41115)	4p16.1	*HMX1*	Yes	200
5	577	NT_016354.16 (9912331–9912907)	4q21.3	*NKX6–1*	Yes	700
6	418	NT_009237.16 (13859103–13859520)	11p15.2	*CALCB*	Yes	50
7	673	NT_011109.15 (19265899–19266571)	19q13.33	*No gene*	Yes	
8	746	NT_022184.13 (23995750–23996496)	2p21	*LOC375201*	Yes	7,600
9	923	NT_026437.10 (32654509–32655429)	14q22.1	*PTGDR*	Yes	40
10	894	NT_008413.16 (37015465–37016356)	9p13	*PAX5*	Yes	8,100
11	533	NT_030059.11 (38044642–38045174)	10q26.1	*EMX2*	Yes	5,300
12	651	NT_010505.14 (1424933–1425583)	16q12.1	*CBLN1*	Yes	680
13	568	NT_007592.13 (1276022–1276589)	6p24	*TFAP2A*	Yes	2,500
14	725	NT_008583.16 (25707371–25708095)	10q22.3	*MGC2555*	Yes	4,500
15	591	NT_079592.1 (49215607–49216197)	7p12.1	*LOC378069*	Yes	190
16	424	NT_023666.16 (1934093–1934516)	8p21.2	*No gene*	Yes	
17	806	NT_009237.16 (30583999–30584804)	11p13	*No gene*	Yes	
18	696	NT_016354.16 (58568060–58568755)	4q28.3	*PCDH10*	Yes	2,500
19	620	NT_079596.1 (7038723–7039342)	7q22	*LAMB1*	Yes	720
20	937	NT_007592.13 (17472263–17473201)	6p21.1	*No gene*	Yes	
21	462	NT_008183.17 (7857852–7858312)	8q11.23	*KIAA1889*	Yes	290
22	487	NT_008470.16 (11911721–11912207)	9q31	*KLF4*	Yes	1,100
23	893	NT_025741.13 (12657384–12658276)	6q21	*NR2E1*	Yes	690
24	750	NT_079592.1 (23721242–23721991)	7p15.1	*NPY*	Yes	370
25	766	NT_077451.3 (1864762–1865527)	5qter	*ADAMTS2*	Yes	1,800
26	607	NT_004610.16 (1272547–1273153)	1p35	*PLA2G2F*	No	2,600
27	404	NT_006713.13 (12160670–12161073)	5q14.3	*CSPG2*	Yes	960
28	521	NT_023666.16 (922959–923479)	8p21.2	*EGR3*	Yes	1,700
29	895	NT_029419.10 (19759986–19760882)	12q13.2	*NXPH4*	No	6,100
30	430	NT_079593.1 (2760886–2761315)	7q11	*No gene*	No	
31	476	NT_011362.8 (4369966–4370441)	20q12	*MAFB*	Yes	350
32	878	NT_033903.6 (11275620–11276497)	11q13.1	*RIN1*	No	550
33	732	NT_009755.16 (3985255–3985983)	12q24.32	*No gene*	Yes	
34	795	NT_026437.10 (16902942–16903736)	14q13	*LOC253970*	Yes	340
35	530	NT_004671.15 (9240059–9240588)	1q31	*LHX9*	Yes	920
36	724	NT_005334.14 (10987626–10988353)	2p24.1	*No gene*	Yes	
37	943	NT_009237.16 (31223373–31224306)	11p13	*WIT-1*	Yes	40
38	587	NT_077921.1 (573714–574300)	1p36.13	*PAX7*	Yes	660
39	273	BX649589.3 (5548–5821)	9q34.3	*AGS3*	Yes	6,100
40	755	NT_022184.13 (8050474–8051228)	2p23.3	*No gene*	No	
41	958	NT_010783.14 (18185717–18186674)	17q22	*TBX4*	Yes	200
42	871	NT_005403.14 (27236075–27236942)	2q31.1	*HOXD3*	Yes	1,300
43	470	NT_030059.11 (21731229–21731698)	10q24	*LBX1*	Yes	5,500
44	406	NT_008818.15 (769699–770104)	10q26.2	*LOC338623*	Yes	230
45	565	NT_023935.16 (8798224–8798788)	9q21	*No gene*	Yes	
46	526	NT_010194.16 (47422212–47422737)	15q23	*ISL2*	Yes	2,700
47	445	NT_029289.10 (9369340–9369784)	5q32	*ADRB2*	Yes	230
48	414	NT_023133.11 (17468804–17469217)	5q34	*NKX2–5*	Yes	2,600
49	583	NT_022792.16 (6841497–6842079)	4q33	*No gene*	Yes	
50	1096	NT_026437.10 (18598721–18599816)	14q13	*SSTR1*	Yes	1,500
51	608	NT_077812.2 (1002922–1003529)	19p13.3	*FLJ46061*	Yes	8,600
52	310	NT_006713.13 (1986840–1987149)	5q13.3	*No gene*	Yes	
53	465	NT_011512.9 (8031349–8031813)	21q21.1	*NCAM2*	Yes	690

Abbreviation: TSS, transcription start site.
* "*No gene*" means TSS of the nearest gene is more than 10 kb away from the isolated region.

tained genes with an expression that was observed in activated T lymphocytes but suppressed in HTLV-I-transformed and ATL cell lines (Fig. 2*A*). On the other hand, the transcription of genes in group II was not detected in activated T cells and HTLV-I-associated cell lines whereas their expression was found in the brain and/or skeletal muscle (Fig. 2*B*). Group II genes were hypermethylated only in ATL cells but not in normal T lymphocytes. These results suggest that the suppressed expression of group I genes is implicated in leukemogenesis.

Relationship between Silencing of Neighboring Genes and DNA Methylation. We studied the detailed DNA methylation status in the promoter and isolated regions of *KLF4* and *EGR3* genes, which belong to group I, using the bisulfite sequencing method. The sequences of each of the 10 clones are summarized in Fig. 3. In both ATL-43T and an acute ATL, the CpGs in the isolated region of *KLF4* gene, which existed in exon 3, were heavily methylated (Fig. 3*A*) whereas there was little methylation in normal PBMCs. In the predicted *KLF4* promoter sequence, there was dense DNA methylation in ATL-43T and mild methylation in fresh ATL cells whereas the CpGs in normal PBMC were little methylated (Fig. 3*A*). DNA methylation in the promoter region of *KLF4* has been studied in primary cells with different stage of ATL to analyze the association with disease progression (Fig. 3*B*). DNA methylation increased according to disease progression from carrier to leukemia although there was little difference between chronic and acute ATL. In the case of the *EGR3* gene, the isolated region, which was in exon 2, was hypermethylated in the ATL cell line and fresh ATL cells but hypomethylated in normal PBMC (Fig. 3*C*). Although the promoter region of *EGR3* was hypermethylated in the ATL cell line, it was not methylated in fresh ATL cells and normal PBMCs.

Next, we analyzed whether the transcriptions of these silenced genes could be recovered by the demethylating agent, 5-aza-dC, and/or a histone deacetylase inhibitor, TSA in ATL cells. The combination of 5-aza-dC and TSA is known to induce a synergistic effect on DNA demethylation (37). As shown in Fig. 2*C*, the transcripts of *KLF4* gene were re-expressed by 5-aza-dC alone or by combination

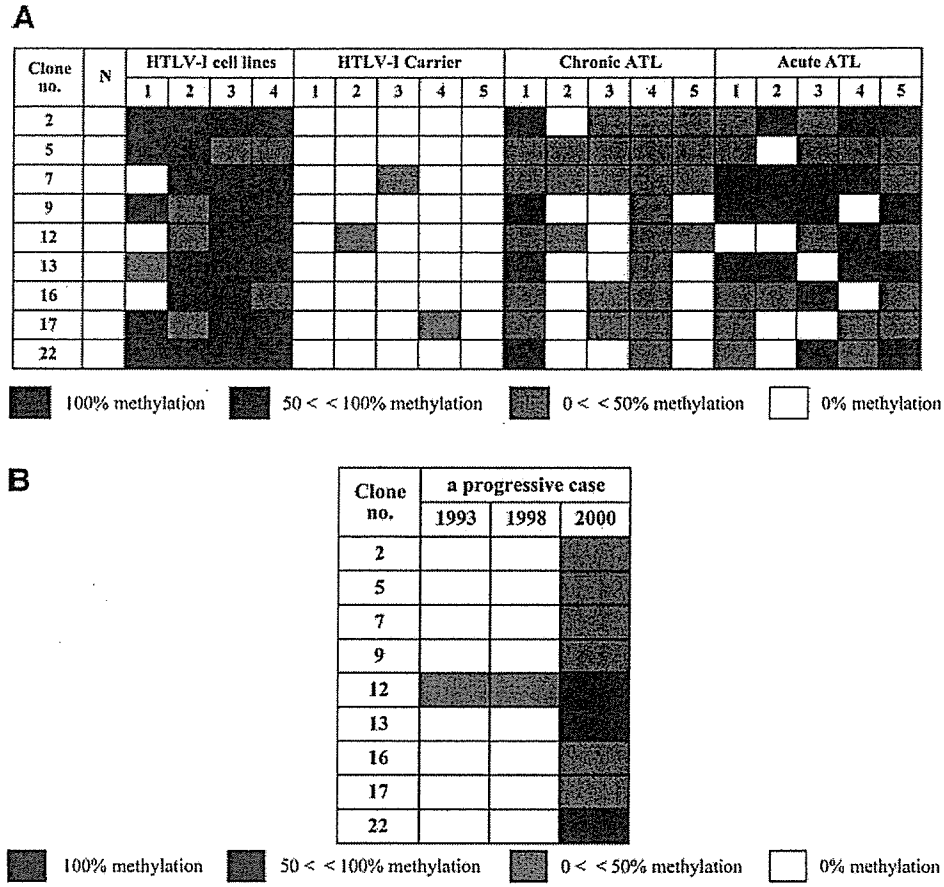

Fig. 1. Frequencies of CpG methylation of the isolated DNA regions in ATL cell lines and clinical samples. The frequencies of CpG methylation in 9 of 53 isolated regions were determined using the Combined Bisulfite Restriction Analysis method. *A*, methylation status in normal PBMCs (N), four ATL cell lines (*1*, MT-1; *2*, ATL-48T; *3*, ATL-43T; *4*, TL-Om1), and PBMCs from five asymptomatic HTLV-I carriers, five chronic ATL, and five acute ATL patients. Densities of methylation are represented by *tones of squares* as presented. *B*, serial changes of methylation status in these regions in a case with progression from carrier state to acute ATL.

treatment but not by TSA alone, suggesting that DNA methylation of *KLF4* gene is associated with its silencing in ATL cells. On the other hand, the transcript of *EGR3* gene was detected more clearly when ATL cells were treated with TSA alone or their combination than with 5-aza-dC alone, indicating that the *EGR3* gene was silenced by histone deacetylation rather than by DNA methylation. However, because demethylation by 5-aza-dC partially recovered *EGR3* gene transcription, we consider that DNA methylation is associated in part with suppressed expression of *EGR3* gene. In addition, the transcriptions of other group I genes, such as *CSPG2*, *MAFB*, and *ADRB2*, were also recovered by 5-aza-dC treatment. Because the transcription of *ADAMTS2* and *PTGDR* could not be recovered by either 5-aza-dC or TSA, the silencing of these genes might be because of other mechanism(s).

Enforced Expression of *KLF4* or *EGR3* Gene in ATL Cells. To investigate the function of *KLF4* and *EGR3* genes in ATL cells, adenovirus vectors expressing *KLF4* (KLF4-AD) or *EGR3* (EGR3-AD), were transfected into ATL-43T, in which the transcription of both genes were completely suppressed. Transfection of *KLF4*-expressing adenovirus vector induced the transcription (Fig. 4*A*) and resulted in accumulation of apoptotic cells as demonstrated by Annexin V-PI staining (Fig. 4*B*). The apoptosis was also confirmed by TUNEL assay (data not shown). The number of apoptotic cells reached maximum 48 hours later (30.1%, Fig. 4*C*). This percentage was similar to that of X-gal-stained cells (49.0%) when lacZ-AD was transfected into ATL-43T. Taken together, these results suggest that *KLF4* expression induced apoptosis in most transduced cells.

Because the *EGR3* gene is reported to be critical for *Fas ligand* (*FasL*) gene transcription (38), we studied whether enforced expression of *EGR3* could induce apoptosis of ATL cells. After transfection, both *EGR3* and *FasL* were transcribed 48 hours later (Fig. 5*A*), which coincided with increased apoptotic cells in ATL-43T infected EGR3-AD, in contrast to control (Fig. 5*B* and *C*). In addition, increased apoptotic cells were also confirmed by TUNEL assay (data not shown). Thus, enforced expression of EGR3 was considered to result in Fas-FasL-mediated apoptosis. To clarify whether this apoptosis is actually mediated by Fas signaling, we transfected vectors expressing $mCasper_L$ or E8. $mCasper_L$ is a mouse c-FLIP that inhibits the activation of procaspase 8 at the death-inducing signaling complex, whereas E8 is a viral FLIP derived from the equine herpes virus type 2. Transfection of EGR3-AD did not increase apoptosis of ATL-43T cells that expressed $mCasper_L$ and E8 (Fig. 5*A* and *C*), confirming that EGR3-induced apoptosis in ATL cell line is mediated by Fas-mediated signal.

DISCUSSION

In the present study, we identified hypermethylated DNA regions by MCA/RDA method. Consistent with the previous study (28), this method could identify hypermethylated CpG islands; 48 of 53 (91%) DNA clones identified in this study satisfied the criteria of CpG islands, and 41 of 53 (77%) DNA clones were located within 10 kb from the transcriptional start site of the nearest gene. Identified genes in the vicinity of isolated hypermethylated DNA regions could be divided into two groups; genes of group II are not expressed and not methylated in normal T lymphocytes, however, are hypermethylated in ATL cells. On the other hand, genes of group I are expressed but not methylated in normal T lymphocytes whereas their expression is suppressed in ATL cells in association with DNA methylation. It is possible that the mechanism of *de novo* methylation is dysregulated,

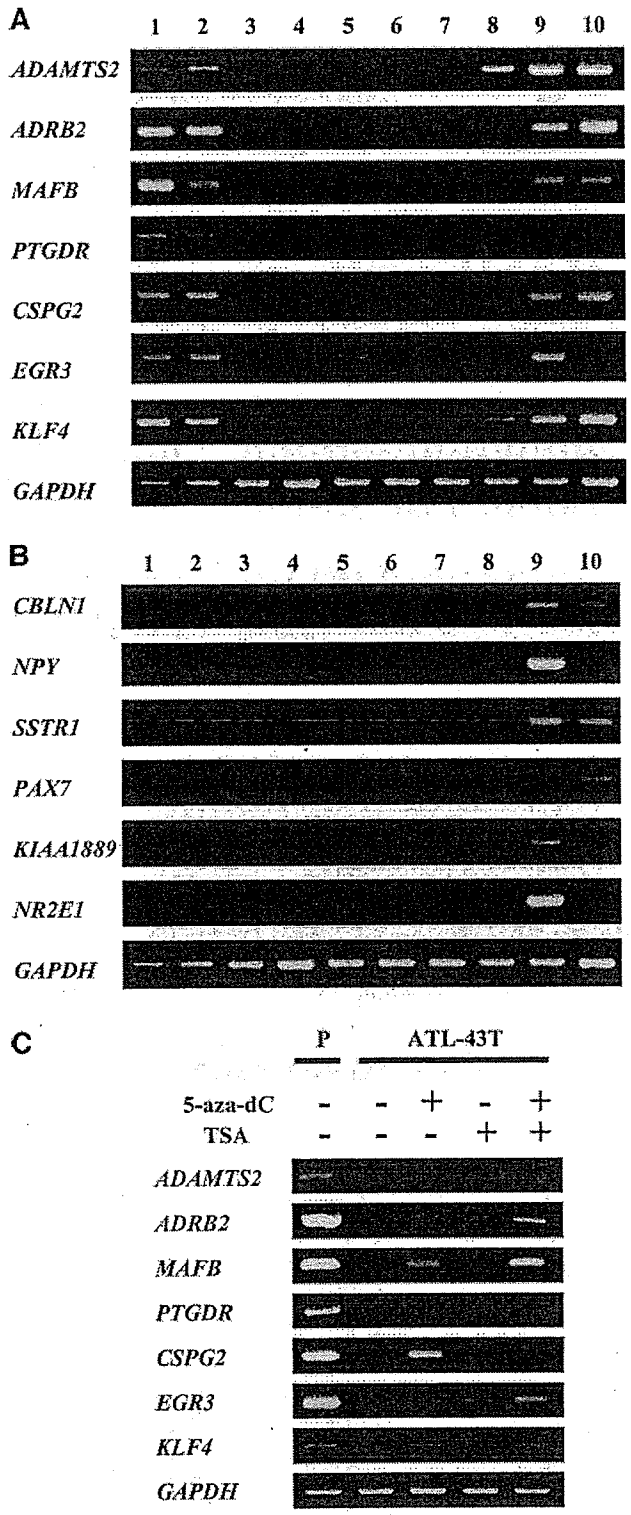

Fig. 2. Expression of genes in the vicinity of hypermethylated regions isolated by MCA/RDA. Expression of the genes near the isolated regions was studied by RT-PCR. Transcripts of the *glyceraldehyde-3-phosphate dehydrogenase* (*GAPDH*) gene were used as a control. *Lane 1*, normal resting PBMC; *Lane 2*, normal activated T cell; *Lane 3*, ED; *Lane 4*, ATL-43T; *Lane 5*, ATL-48T; *Lane 6*, ATL-55T; *Lane 7*, MT-1; *Lane 8*, MT-2; *Lane 9*, normal whole brain; *Lane 10*, normal skeletal muscle. *A*, group I, genes expressed in normal T cells but suppressed in HTLV-I-transformed and ATL cell lines. *B*, group II, genes not expressed in normal T cells and HTLV-I-associated cell lines. *C*, recovered expression of the group I genes after demethylation, ATL-43T was treated with 5-aza-dC only, TSA only, or both. Using cDNAs obtained from the treated and untreated cells, expressions of *KLF4* and *EGR3* were analyzed by RT-PCR. Phytohemagglutinin blast (P) was used as a positive control. RT-PCR of *GAPDH* was also performed to provide a control for initial RNA amounts.

resulting in aberrant methylation of genes despite their transcription as observed in group II genes. In this regard, Toyota *et al.* (28) isolated 33 hypermethylated DNA sequences in a colon cancer cell line using the MCA/RDA method and named these clones MINT1–33. Among DNA regions identified in this study, four clones were identical to MINT clones (Table 1, clone 2, clone 15, clone 30 and clone 48). These findings indicate that such DNA regions in the genome are prone to be methylated in cancer cells, which is consistent with an earlier report (22), although the factors that determine such susceptibility to methylation remain unresolved. In addition to such DNA methylation observed among different types of cancer cells, there are hypermethylated genes specifically observed in ATL cells. Analysis of DNA methylation of such genes in non-ATL T-cell lines showed that they were also methylated (data not shown), suggesting that DNA methylation of such genes is T-cell specific.

In addition to hypermethylation, we also reported hypomethylated genes in ATL cells, which included *MEL1S*, *CACNA1H*, and *Nogo receptor* genes as identified by the MCA/RDA method (30). Among them, the aberrant expression of *MEL1S* was frequently observed in ATL cells and has been shown to confer resistance against transforming growth factor-β. Thus, the MCA/RDA method indicates the involvement of both hyper- and hypomethylation in leukemogenesis of ATL although in a different manner.

In the case of *EGR3* gene, only the coding regions were methylated with little DNA methylation of the promoter region in fresh ATL cells although its expression was suppressed. TSA has more profound effect than 5-aza-dC, suggesting that histone modification, rather than DNA methylation, in the promoter region might silence the transcription of the *EGR3* gene. However, because DNA methylation in the coding region was associated with such silencing, detection of DNA methylation in non-promoter regions is also capable of identifying such silenced genes as observed in the *EGR3* gene.

EGR3 is a transcriptional factor containing zinc finger domain as well as KLF4. It has been reported that enforced expression of *EGR3* gene resulted in expression of *FasL* in HeLa cells (38), indicating that EGR3 is a critical transcriptional factor for *FasL* transcription. In agreement with these results, we also showed that expression of *EGR3* induced *FasL* transcription, resulting in apoptosis of ATL cells. Although ATL cells possess a phenotype of activated T cells and highly express Fas antigens on their surfaces, they do not produce FasL. On the other hand, normal T lymphocytes can express both Fas antigens and FasL after activation, and the number of activated T lymphocytes is regulated by Fas-FasL system-mediated apoptosis, which is designated as activation-induced cell death (39). Activation-induced cell death controls the number of activated T lymphocytes, consequently suppressing the immune response. Suppression of *EGR3* gene in ATL cells could account for lack of expression of FasL, which enables ATL cells to escape from activation-induced cell death. In the present study, we demonstrated that enforced expression of *EGR3* gene-induced FasL expression and apoptosis. Thus, because both KLF4 and EGR3 are accelerators of ATL cell apoptosis, *KLF4* and *EGR3* genes are considered new tumor-suppressor gene candidates in ATL.

KLF4 is a member of the Kruppel-like factor family, which is highly expressed in epithelial tissues such as the gut and skin, especially in the terminally differentiated cells (40, 41). Previous studies reported that KLF4 plays important roles in the regulation of G_1-S and G_2-M cell cycle checkpoint in colon cancer cells and that these functions are likely to be p53-dependent (42–44). According to these findings, KLF4 is thought to be associated with tumorigenicity of colon cancer cells. However, there is no report regarding the functional role of *KLF4* gene in lymphoid cells. Our study demonstrated that KLF4 expression induced apoptosis of ATL cells. Although the

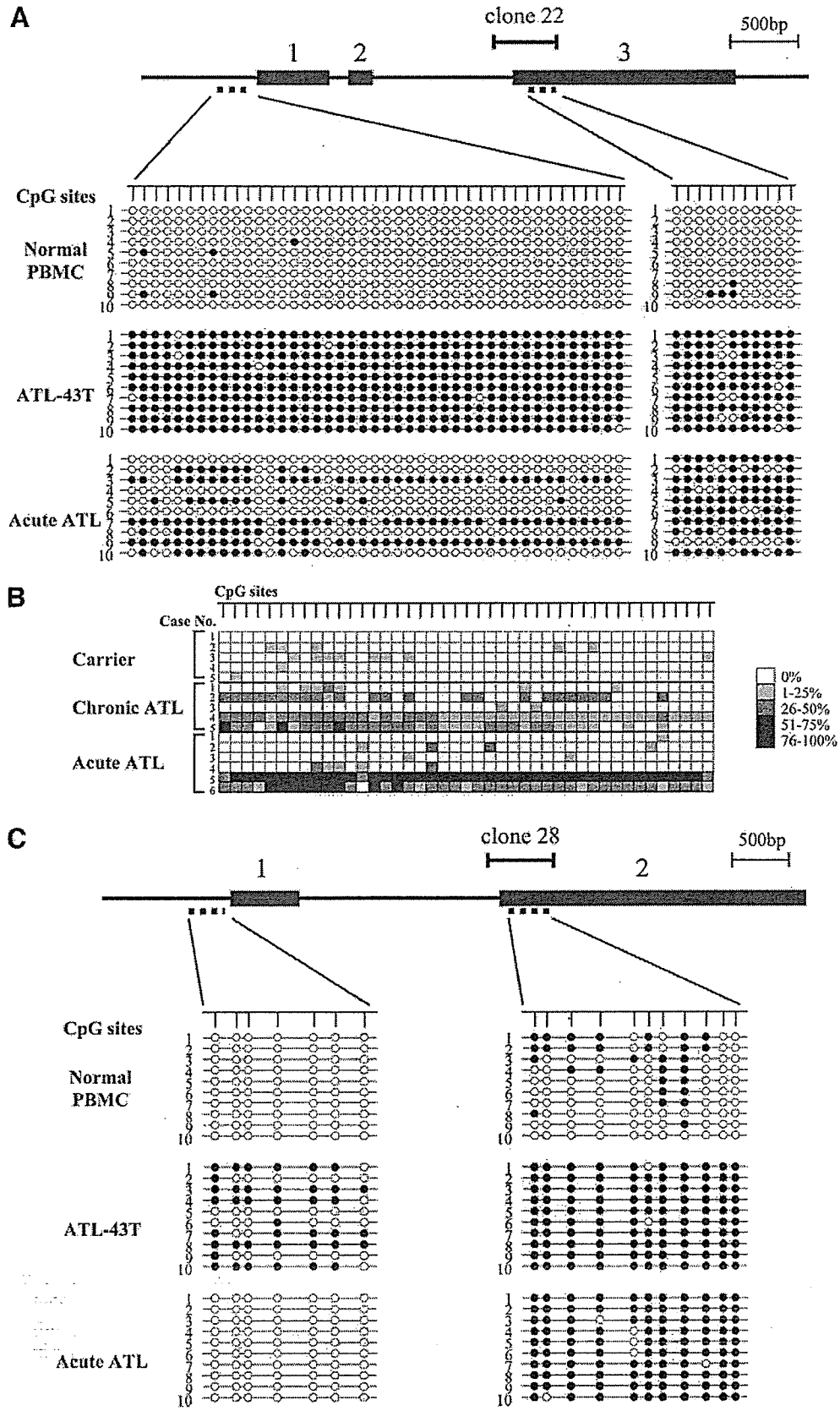

Fig. 3. Methylation status of *KLF4* and *EGR3* genes. Genomic DNAs of normal PBMC, an ATL cell line (ATL-43T), and primary cells of acute ATL were treated by sodium bisulfite and then amplified by primers specific for DNA regions in *KLF4* and *EGR3* genes identified by MCA/RDA and for their promoter regions. Then, PCR products were subcloned into plasmid DNA, and the sequences were determined in 10 clones of each (*A*, *KLF4*; *C*, *EGR3*). ○, unmethylated CpG sites; ●, methylated CpG sites. *B*, methylation status of *KLF4* promoter in primary cells with different stage of ATL; methylation level of each CpG site was calculated based on the results of bisulfite sequencing analysis and represented by *tones of squares*.

mechanism of apoptosis needs additional study, its silencing by DNA methylation facilitates the survival of ATL cells.

The present study showed that the densities of CpG methylation in identified DNA regions tend to increase with disease progression. Moreover, analysis of sequential samples from a patient who was followed from carrier state until the onset of acute ATL revealed that DNA methylation accumulated at the onset of ATL (Fig. 1*B*). These data indicate that serial analysis of the methylation status in identified hypermethylated regions might be a useful tool in the diagnosis and staging of ATL.

HTLV-I-infected clones have been shown to persist over seven years in the same HTLV-I carrier (45), suggesting that HTLV-I-infected cells survive for a long time through the action of viral proteins. On the other hand, it has been reported that aging is closely related to alterations of DNA methylation. Progressive loss of 5-methylcytosine content is observed in normal aging cells, primarily within DNA-repeated sequences. In contrast, some genes show progressive, age-related increases of DNA methylation, resulting in silencing their expressions (46). Taken together, the prolonged life span of HTLV-I-infected T cells might be a predisposing factor for aberrant DNA methylation. During the long latent period, it is possible that HTLV-I-infected cells that are adapted for survival are selected *in vivo*. In such evolution of infected cells, genetic and epigenetic changes are thought to play critical roles by suppressing the transcription of genes with tumor suppressor functions or activating the expression of genes, which exerts positive effects on survival of tumor cells.

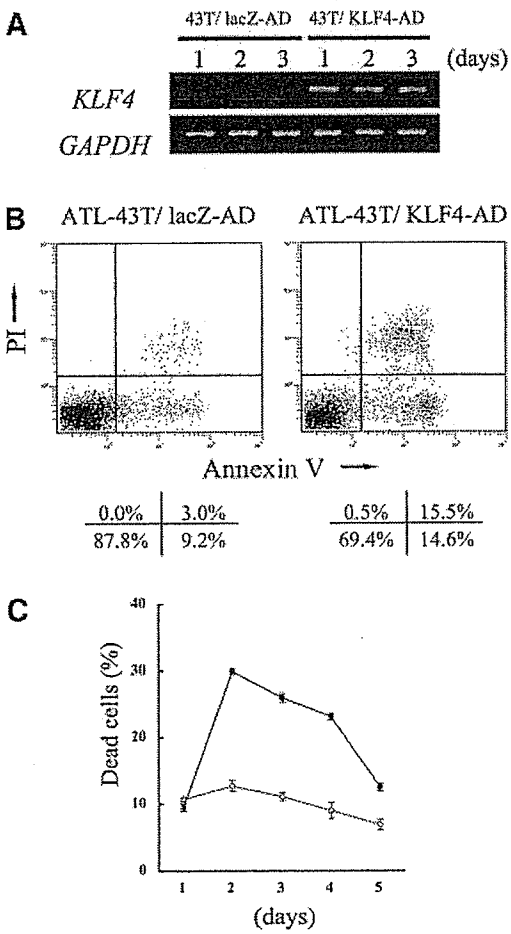

Fig. 4. Induction of apoptosis of ATL-43T by enforced expression of *KLF4*. *A*, expression of *KLF4* gene in ATL-43T transfected with lacZ-AD or KLF4-AD was studied by RT-PCR. *B*, detection of apoptotic cells in ATL-43T by double staining with Annexin V-FITC and PI at day 2 of lacZ-AD and KLF4-AD infection. The percentage of cells in each quadrant is shown at the *bottom of the panels*. *C*, serial changes in the percentages of dead cells detected by Annexin V-PI double staining. ○, ATL-43T infected with lacZ-AD; ●, ATL-43T infected with KLF4-AD. Data are mean ± SE.

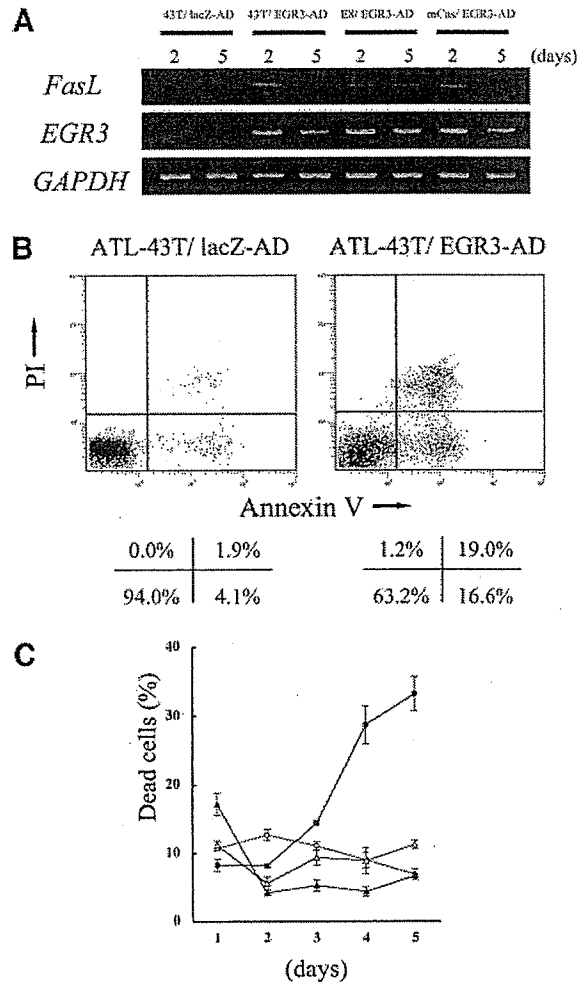

Fig. 5. Induction of *FasL* transcription and apoptosis of ATL-43T by enforced expression of *EGR3*. *A*, expressions of *EGR3* and *FasL* genes in transfected cell lines were studied by RT-PCR. *B*, detection of apoptotic cells in ATL-43T by double staining with Annexin V-FITC and PI at day 5 of lacZ-AD and EGR3-AD infection. The percentage of cells in each quadrant is shown at the *bottom of the panels*. *C*, serial changes in the percentages of dead cells detected by Annexin V-PI double staining. ○, ATL-43T infected with lacZ-AD; ●, ATL-43T infected with EGR3-AD; △, ATL-43T-mCas infected with EGR3-AD; and ▲, ATL-43T-E8 infected with EGR3-AD. Data are mean ± SE.

In conclusion, we have demonstrated in the present study that the MCA/RDA method could identify the differentially methylated DNA regions and genes according to disease progression of ATL. Such identification of aberrantly methylated genes allows for the diagnosis and staging of ATL and clarifies the molecular mechanism of leukemogenesis.

ACKNOWLEDGMENTS

We are grateful to Michiyuki Maeda for providing us valuable cell lines and to Yoshihiro Koya for valuable help. The authors also thank Dr. F. G. Issa (word-medex.com.au) for careful reading and editing of the manuscript.

REFERENCES

1. Takatsuki K, Uchiyama T, Sagawa K, Yodoi J. Adult T cell leukemia in Japan. In: Seno S, Takaku F, Irino S, editors. Topic in hematology: proceedings of the 16th international congress of Hematology, Kyoto, September 5–11, 1976. Amsterdam, Oxford: Excerpta Medica; 1977. p. 73–7.

2. Uchiyama T, Yodoi J, Sagawa K, Takatsuki K, Uchino H. Adult T-cell leukemia: clinical and hematologic features of 16 cases. Blood 1977;50:481–92.
3. Poiesz BJ, Ruscetti FW, Gazdar AF, Bunn PA, Minna JD, Gallo RC. Detection and isolation of type C retrovirus particles from fresh and cultured lymphocytes of a patient with cutaneous T-cell lymphoma. Proc Natl Acad Sci USA 1980;77:7415–9.
4. Wong-Staal F, Gallo RC. Human T-lymphotropic retroviruses. Nature (Lond) 1985; 317:395–403.
5. Arisawa K, Soda M, Endo S, et al. Evaluation of adult T-cell leukemia/lymphoma incidence and its impact on non-Hodgkin lymphoma incidence in southwestern Japan. Int J Cancer 2000;85:319–24.
6. Yoshida M. Multiple viral strategies of HTLV-1 for dysregulation of cell growth control. Annu Rev Immunol 2001;19 475–96.
7. Franchini G, Fukumoto R, Fullen JR. T-cell control by human T-cell leukemia/ lymphoma virus type 1. Int J Hematol 2003;78:280–96.
8. Jeang KT. Functional activities of the human T-cell leukemia virus type I Tax oncoprotein: cellular signaling through NF-kappa B. Cytokine Growth Factor Rev 2001;12:207–17.
9. Fujii M, Tsuchiya H, Chuhjo T, Akizawa T, Seiki M. Interaction of HTLV-1 Tax1 with p67SRF causes the aberrant induction of cellular immediate early genes through CArG boxes. Genes Dev 1992;6:2066–76.
10. Kwok RP, Laurance ME, Lundblad JR, et al. Control of cAMP-regulated enhancers by the viral transactivator Tax through CREB and the co-activator CBP. Nature (Lond) 1996;380:642–6.
11. Jeang KT, Widen SG, Semmes OJ 4th, Wilson SH. HTLV-I trans-activator protein, tax, is a trans-repressor of the human beta-polymerase gene. Science (Wash D C) 1990;247:1082–4.
12. Suzuki T, Uchida-Toita M, Yoshida M. Tax protein of HTLV-1 inhibits CBP/p300-mediated transcription by interfering with recruitment of CBP/p300 onto DNA element of E-box or p53 binding site. Oncogene 1999;18:4137–43.
13. Jin DY, Spencer F, Jeang KT. Human T cell leukemia virus type 1 oncoprotein Tax targets the human mitotic checkpoint protein MAD1. Cell 1998;93:81–91.
14. Takeda S, Maeda M, Morikawa S, et al. Genetic and epigenetic inactivation of tax gene in adult T-cell leukemia cells. Int J Cancer 2004;109:559–67.
15. Tamiya S, Matsuoka M, Etoh K, et al. Two types of defective human T-lymphotropic virus type I provirus in adult T-cell leukemia. Blood 1996;88:3065–73.
16. Furukawa Y, Kubota R, Tara M, Izumo S, Osame M. Existence of escape mutant in HTLV-I tax during the development of adult T-cell leukemia. Blood 2001;97:987–93.
17. Koiwa T, Hamano-Usami A, Ishida T, et al. 5'-long terminal repeat-selective CpG methylation of latent human T-cell leukemia virus type 1 provirus in vitro and in vivo. J Virol 2002;76:9389–97.
18. Bangham CR. Human T-lymphotropic virus type 1 (HTLV-1): persistence and immune control. Int J Hematol 2003;78:297–303.
19. Sakashita A, Hattori T, Miller CW, et al. Mutations of the p53 gene in adult T-cell leukemia. Blood 1992;79:477–80.
20. Hatta Y, Hirama T, Miller CW, Yamada Y, Tomonaga M, Koeffler HP. Homozygous deletions of the p15 (MTS2) and p16 (CDKN2/MTS1) genes in adult T-cell leukemia. Blood 1995;85:2699–704.
21. Nosaka K, Maeda M, Tamiya S, Sakai T, Mitsuya H, Matsuoka M. Increasing methylation of the CDKN2A gene is associated with the progression of adult T-cell leukemia. Cancer Res 2000;60:1043–8.
22. Costello JF, Fruhwald MC, Smiraglia DJ, et al. Aberrant CpG-island methylation has non-random and tumour-type-specific patterns. Nat Genet 2000;24:132–8.
23. Esteller M, Corn PG, Baylin SB, Herman JG. A gene hypermethylation profile of human cancer. Cancer Res 2001;61:3225–9.
24. Hayashizaki Y, Hirotsune S, Okazaki Y, et al. Restriction landmark genomic scanning method and its various applications. Electrophoresis 1993;14:251–8.
25. Gonzalgo ML, Liang G, Spruck CH, 3rd, Zingg JM, Rideout WM, 3rd, Jones PA. Identification and characterization of differentially methylated regions of genomic DNA by methylation-sensitive arbitrarily primed PCR. Cancer Res 1997;57:594–9.
26. Ushijima T, Morimura K, Hosoya Y, et al. Establishment of methylation-sensitive-representational difference analysis and isolation of hypo- and hypermethylated genomic fragments in mouse liver tumors. Proc Natl Acad Sci USA 1997;94:2284–9.
27. Huang TH, Laux DE, Hamlin BC, Tran P, Tran H, Lubahn DB. Identification of DNA methylation markers for human breast carcinomas using the methylation-sensitive restriction fingerprinting technique. Cancer Res 1997;57:1030–4.
28. Toyota M, Ho C, Ahuja N, et al. Identification of differentially methylated sequences in colorectal cancer by methylated CpG island amplification. Cancer Res 1999;59: 2307–12.
29. Ballestar E, Paz MF, Valle L, et al. Methyl-CpG binding proteins identify novel sites of epigenetic inactivation in human cancer. EMBO J 2003;22:6335–45.
30. Yoshida M, Nosaka K, Yasunaga J, Nishikata I, Morishita K, Matsuoka M. Aberrant expression of the MEL1S gene identified in association with hypomethylation in adult T-cell leukemia cells. Blood 2004;103:2753–60.
31. OhYama T, Tsukumo S, Yajima N, Sakamaki K, Yonehara S. Reduction of thymocyte numbers in transgenic mice expressing viral FLICE-inhibitory protein in a Fas-independent manner. Microbiol Immunol 2000;44:289–97.
32. Krueger A, Schmitz I, Baumann S, Krammer PH, Kirchhoff S. Cellular FLICE-inhibitory protein splice variants inhibit different steps of caspase-8 activation at the CD95 death-inducing signaling complex. J Biol Chem 2001;276:20633–40.
33. Xiong Z, Laird PW. COBRA: a sensitive and quantitative DNA methylation assay. Nucleic Acids Res 1997;25:2532–4.
34. Clark SJ, Harrison J, Paul CL, Frommer M. High sensitivity mapping of methylated cytosines. Nucleic Acids Res 1994;22:2990–7.
35. Takai D, Jones PA. Comprehensive analysis of CpG islands in human chromosomes 21 and 22. Proc Natl Acad Sci USA 2002;99:3740–5.
36. Palmisano WA, Crume KP, Grimes MJ, et al. Aberrant promoter methylation of the transcription factor genes PAX5 alpha and beta in human cancers. Cancer Res 2003;63:4620–5.
37. Cameron EE, Bachman KE, Myohanen S, Herman JG, Baylin SB. Synergy of demethylation and histone deacetylase inhibition in the re-expression of genes silenced in cancer. Nat Genet 1999;21:103–7.
38. Mittelstadt PR, Ashwell JD. Cyclosporin A-sensitive transcription factor Egr-3 regulates Fas ligand expression. Mol Cell Biol 1998;18:3744–51.
39. Krammer PH. CD95's deadly mission in the immune system. Nature (Lond) 2000; 407:789–95.
40. Shields JM, Christy RJ, Yang VW. Identification and characterization of a gene encoding a gut-enriched Kruppel-like factor expressed during growth arrest. J Biol Chem 1996;271:20009–17.
41. Segre JA, Bauer C, Fuchs E. Klf4 is a transcription factor required for establishing the barrier function of the skin. Nat Genet 1999;22:356–60.
42. Zhang W, Geiman DE, Shields JM, et al. The gut-enriched Kruppel-like factor (Kruppel-like factor 4) mediates the transactivating effect of p53 on the p21WAF1/ Cip1 promoter. J Biol Chem 2000;275:18391–8.
43. Yoon HS, Chen X, Yang VW. Kruppel-like factor 4 mediates p53-dependent G1/S cell cycle arrest in response to DNA damage. J Biol Chem 2003;278:2101–5.
44. Yoon HS, Yang VW. Requirement of Kruppel-like factor 4 in preventing entry into mitosis following DNA damage. J Biol Chem 2004;279:5035–41.
45. Etoh K, Tamiya S, Yamaguchi K, et al. Persistent clonal proliferation of human T-lymphotropic virus type I-infected cells in vivo. Cancer Res 1997;57:4862–7.
46. Issa JP. Age-related epigenetic changes and the immune system. Clin Immunol 2003;109:103–8.

Aberrant expression of the *MEL1S* gene identified in association with hypomethylation in adult T-cell leukemia cells

Mika Yoshida, Kisato Nosaka, Jun-ichirou Yasunaga, Ichiro Nishikata, Kazuhiro Morishita, and Masao Matsuoka

DNA methylation plays critical roles in the development and differentiation of mammalian cells, and its dysregulation has been implicated in oncogenesis. This study was designed to determine whether DNA hypomethylation–associated aberrant gene expression is involved in adult T-cell leukemia (ATL) leukemogenesis. We isolated hypomethylated DNA regions of ATL cells compared with peripheral blood mononuclear cells from a carrier by a methylated CpG-island amplification/representational difference analysis method. The DNA regions identified contained *MEL1*, *CACNA1H*, and *Nogo receptor* genes. Sequencing using sodium bisulfite–treated genomic DNAs revealed the decreased methylated CpG sites, confirming that this method detected hypomethylated DNA regions. Moreover, these hypomethylated genes were aberrantly transcribed. Among them, *MEL1S*, an alternatively spliced form of *MEL1* lacking the PR (positive regulatory domain I binding factor 1 and retinoblastoma-interacting zinc finger protein) domain, was frequently transcribed in ATL cells, and the transcriptional initiation sites were identified upstream from exons 4 and 6. Transfection of *MEL1S* into CTLL-2 cells conferred resistance against transforming growth factor β (TGF-β), suggesting that aberrant expression of *MEL1S* was associated with dysregulation of TGF-β–mediated signaling. Although Tax renders cells resistant to TGF-β, Tax could not be produced in most fresh ATL cells, in which *MEL1S* might be responsible for TGF-β resistance. Our results suggest that aberrant gene expression associated with DNA hypomethylation is implicated in leukemogenesis of ATL. (Blood. 2004;103:2753-2760)

Introduction

Adult T-cell leukemia (ATL) is a neoplastic disease of $CD4^+$ T lymphocytes that is etiologically associated with human T-cell leukemia virus type I (HTLV-I).[1-6] After transmission, HTLV-I increases the number of infected cells through its viral proteins, including Tax. Tax encoded by the pX region between *env* and the 3′ long terminal repeat (LTR) is an oncoprotein with pleiotropic actions,[7,8] including transactivation of the nuclear factor kappaB (NFκB), serum responsive factor (SRF), and cyclic adenosine monophosphate (cAMP) response element-binding protein (CREB) pathways; transrepression of genes, such as DNA polymerase β, *lck*, and *p18* genes; and functional inactivation of p53, p16, and mitotic arrest-defective 1 (MAD1).[8,9] With these actions, Tax promotes the proliferation and inhibits apoptosis of infected cells, resulting in their clonal expansion and increased proviral load.

The cumulative risk of developing ATL after HTLV-I infection was estimated to be 6% in men and 2% in women.[10] In addition, there is a long latent period before the onset of ATL, suggesting that additional factors other than viral proteins are implicated in leukemogenesis. Although somatic changes of genes, such as mutation of *p53*[11] or deletion of *p16*,[12] were reported in ATL, they were not so frequent in ATL cells and were predominantly observed in aggressive forms of ATL, such as acute and lymphoma types. This suggested that these genetic changes were implicated in the progression of ATL. In addition, it has been reported that DNA methylation of the *p16* gene silenced its expression, indicating that epigenetic changes were also implicated in leukemogenesis.[13]

Epigenetic changes include dysregulated DNA methylation in cancer cells, which consists of hypermethylation and hypomethylation of DNA.[14] Hypermethylation is frequently associated with gene silencing when hypermethylation occurs in the promoter region of genes.[15] The same mechanism is considered to regulate the transcriptional silencing of various tumor suppressor genes, including *p16*,[16] *p15*,[17] *hMLH1*,[18] *BRCA1*,[19] and *GSTP1* genes.[20] From the perspective of the whole genome, genome-wide hypomethylation has been reported in cancer cells,[21-23] and demethylation due to decreased expression of DNA methyltransferase has been shown to be associated with oncogenesis.[24] Two mechanisms by which DNA hypomethylation is associated with oncogenesis have been considered: (1) DNA hypomethylation directly induces genetic instability, and (2) aberrant transcription is linked with DNA hypomethylation. In the immunodeficiency, centromeric instability, and facial anomalies (ICF) syndrome, the underlying abnormalities are mutations of both alleles of the gene that encodes DNA methyltransferase 3B (Dnmt3B).[25,26] Chromosomal instability has also been demonstrated in mice with decreased expression of Dnmt1.[24] Taken together, these findings suggest that undermethylation of the CpG sites is closely linked with organization and stabilization of chromatin structures. Although DNA hypomethylation in cancer cells was frequently observed in both highly and

From the Laboratory of Virus Immunology, Institute for Virus Research, Kyoto University, Kyoto, Japan; Division of Tumor Biochemistry, Department of Biochemistry, Miyazaki Medical College, University of Miyazaki, Miyazaki, Japan.

Submitted July 23, 2003; accepted November 17, 2003. Prepublished online as *Blood* First Edition Paper, December 4, 2003; DOI 10.1182/blood-2003-07-2482.

Supported by a Grant-in-aid for Scientific Research from the Ministry of Education, Science, Sports, and Culture of Japan.

Reprints: Masao Matsuoka, Laboratory of Virus Immunology, Institute of Virus Research, Kyoto University, Kyoto 606-8507, Japan; e-mail: mmatsuok@virus.kyoto-u.ac.jp.

The publication costs of this article were defrayed in part by page charge payment. Therefore, and solely to indicate this fact, this article is hereby marked "advertisement" in accordance with 18 U.S.C. section 1734.

moderately repetitive DNA sequences,[14] it was also detected in transcriptional units of single-copy genes. Such genes included *MAGE-1*,[27] *MDR1*,[28] and *HOX11*.[29]

The present study was designed to determine the DNA methylation status in ATL and whether DNA hypomethylation–associated aberrant gene expression is involved in ATL leukemogenesis. We report the isolation of hypomethylated DNA regions from ATL cells compared with cells in the carrier state by the methylated CpG-island amplification/representational difference analysis (MCA/RDA) method and identification of hypomethylated and aberrantly expressed genes in ATL cells.

Materials and methods

Cell lines and antibody

HTLV-I–transformed cell lines and ATL-derived cell lines used in this study were as follows: ATL-43T, ATL-55T, ED, and ATL-2 were cell lines derived from leukemic clones,[13] and MT-4 and ATL-35T were derived from nonleukemic clones. Hut78, Jurkat, SupT1, and Kit225 were T-cell lines not associated with HTLV-I. The human embryonic kidney cell line, 293, was used as a control. Rabbit serum anti–MDS1/EVI1-like gene 1 (anti-MEL1) DNA binding domain 2 (nucleotides [nt's] 2613-3152) was prepared as described previously.[30]

MCA/RDA

MCA/RDA was performed as described previously.[31] For preparation of MCA/RDA amplicons, genomic DNA extracted from peripheral blood mononuclear cells of an HTLV-I carrier was used as a tester and that from acute ATL cells was used as a driver. Five micrograms of DNA was digested with 110 units of *Sma*I overnight. The DNA was then digested with 20 units of *Xma*I overnight. DNA fragments were then precipitated with ethanol. The RMCA polymerase chain reaction (PCR) adaptor was prepared by incubation of 2 oligonucleotides RMCA24 (5′-CCACCGCCATCCGAGCCTTTCTGC-3′) and RMCA12 (5′-CCGGGCAGAAAG-3′) at 65°C for 2 minutes, followed by cooling to room temperature. DNA (0.5 μg) was ligated to 0.5 nmol of RMCA adaptor using T4 DNA ligase. PCR was performed using 2 μL of each of ligation mix as a template in a 100-μL volume containing 100 pmol RMCA24 primer, 2 units of ExTaq (Takara, Shiga, Japan), 2 mM $MgCl_2$, 16 mM $NH_4(SO_4)_2$, 10 μg/mL bovine serum albumin (BSA), and 5% vol/vol dimethyl sulfoxide (DMSO). The reaction mixture was incubated at 72°C for 5 minutes and 95°C for 3 minutes. Samples were then subjected to 25 cycles amplification consisting of 1 minute at 95°C and 3 minutes at 77°C in a thermal cycler (Perkin Elmer Applied Biosystems, Norwalk, CT). The final extension time was 10 minutes. All restriction enzymes and T4 DNA ligase were from New England Biolabs (Beverly, MA). In the RDA step, 500 ng and 100 ng of ligation mixture were used for the first and second competitive hybridization, respectively. To eliminate the digested adaptor, CHROMA SPIN Column (BD Biosciences Clontech, Palo Alto, CA) was used. Primers used for the first and second rounds of RDA were as follows: JMCA24, 5′-GTGAGGGTCGGATCTGGATGGCTC-3′; JMCA12, 5′CCGGGAGCCAGC-3′; NMCA24, 5′-GTTAGCGGACACAGGGCGGGTCAC-3′; and NMCA12, 5′-CCGGGTGACCCG. After the second round of competitive hybridization, the PCR products were subcloned into pCR-XL-TOPO (Invitrogen, Carlsbad, CA), and then the insert of each clone was amplified with M13 forward (M13F) (5′-CCCAGTCACGACGTTGTAAAACGA-3′), and M13 reverse (M13R) (5′-AGCGGATAACAATTTCACACAGGA-3′) primers. Sequence analysis was carried out using automated DNA sequencers (Perkin Elmer Applied Biosystems). Sequence homologies were identified using the BLAST program of the National Center for Biotechnology Information available at http://www.ncbi.nlm.nih.gov:80/BLAST/.

Southern blot analysis

To confirm that the MCA/RDA method isolated hypomethylated DNA fragments, we performed Southern blot analysis using the isolated DNA fragments as probes. Tester and driver MCA amplicons (500 ng each) were separated by electrophoresis in an agarose gel and transferred to a positive charge nylon membrane (Hybond-N; Amersham Biosciences, Piscataway, NJ). Filters were hybridized with alkaline phosphatase–labeled probes and then washed using Alphos Direct Labeling and Detection with CDP-Star (Amersham Biosciences). Filters were then exposed to film (Medical X-ray film; Kodak, Rochester, NY) for a few seconds and analyzed.

Direct sequencing after sodium bisulfite treatment

One microgram of genomic DNA (10 μL) was denatured by the addition of an equal volume of 0.6 N NaOH for 15 minutes and then 208 μL of 3.6 M sodium bisulfite and 12 μL of 10 mM hydroxyquinone were added. This mixture was incubated at 55°C for 16 hours to convert cytosine to uracil. Treated genomic DNA was subsequently purified using the Wizard clean-up system (Promega, Madison, WI), precipitated with ethanol, and resuspended in 100 μL of dH_2O. Sodium bisulfite–treated genomic DNAs (50 ng) were amplified with the specific primers to isolated DNA regions, and then PCR products were subcloned into plasmid DNA. Sequences of 10 clones of each were determined using Big Dye Terminator (Perkin Elmer Applied Biosystems) with an ABI 377 autosequencer.

Synthesis of cDNA and semiquantitative reverse transcriptase (RT)–PCR

Transcripts of *MEL, CACNA1H,* and *Nogo receptor* genes were quantified using semiquantitative RT-PCR as described previously.[32] Total RNA was extracted from each sample using TRIZOL (Invitrogen), and cDNA was synthesized from 1 to 5 μg of total RNAs by the Superscript Preamplification System (Invitrogen) according to the protocol recommended by the manufacturer. PCR was performed using 1 μL of reverse transcriptase reaction sample mixed with 50 μL of PCR reaction buffer containing 0.2 mM each of deoxynucleotide triphosphate, 2 mM $MgCl_2$, 1.25 units of ExTaq polymerase (Takara), and 0.5 μM of each primer using the hot start technique with AmpliWax PCR Gem 100 (Perkin Elmer Applied Biosystems). Primers were 5′-AGTGAGATGAACCAAGCATCAACG-3′ (sense), 5′-CTGCACAGTGTATGTTTTAAAGCC-3′ (antisense) for *MEL1/1S;* 5′-TGTGACGAGTGTGACGAACT-3′ (sense), 5′-GTTTTCACATTCGAAGCGTT-3′ (antisense) for *MEL1S;* 5′-CCCTGTCTACATTCCTGAAG-3′ (sense), 5′-CCACGTCCGTCAGTATTTGC-3′ (antisense) for *MEL1;* 5′-CGCCACCTTCAGCAACTTCGGCAT-3′ (sense), 5′-ATCTCCACCTCCTGCAGCGG-3′ (antisense) for *CACNA1H;* and 5′-CAGTACCTGAGGCTCAACGACAAC-3′ (sense), 5′-ACCTGAGCCTTCTGAGTCACCAGT-3′ (antisense) for *Nogo receptor* in T-Gradient Thermocycler (Biometra, Gottingen, Germany). The PCRs were performed under the following conditions: *MEL1/1S:* 2 minutes at 94°C, for 36 cycles for 30 seconds at 94°C, 30 seconds at 56°C, 30 seconds at 72°C; *MEL1* and *MEL1S:* 2 minutes at 94°C, for 40 cycles for 30 seconds at 94°C, 30 seconds at 58°C, 30 seconds at 72°C; *CACNA1H:* 2 minutes at 94°C, for 40 cycles for 30 seconds at 94°C, 30 seconds at 60°C, 30 seconds at 72°C; and *Nogo receptor:* 3 minutes at 94°C, for 40 cycles for 1 minute at 94°C, 40 seconds at 57°C, and 50 seconds at 72°C.

Western blot analysis

Cells were lysed in a buffer containing 20 mM Tris-HCl (pH 8.0), 150 mM NaCl, 1% Triton X, 10% glycerol, 0.5 mM dithiothreitol (DTT), 0.5 mM phenylmethylsulfonyl fluoride (PMSF), 1 mM Na_3VO_4, 10 μg/mL aprotinin, and 10 μg/mL leupeptin. After 30 minutes on ice, lysates were cleared by centrifugation at 12 500*g* (15 000 rpm) for 15 minutes at 4°C. Proteins (20 μg) were separated by sodium dodecyl sulfate–polyacrylamide gel electrophoresis (SDS-PAGE) followed by electrotransfer to a polyvinylidene difluoride membrane (ATTO, Tokyo, Japan). The blots were blocked in blocking buffer for 1 hour at room temperature and incubated in 3000-fold diluted rabbit serum anti-MEL1 DNA binding domain 2 for 1 hour at room temperature. After 5 washes in 0.5% Tween–phosphate-buffered saline (PBS), the blots were incubated in 4000-fold diluted antirabbit immunoglobulin-biotinylated specific whole antibody (from donkey) (Amersham Biosciences) for 30 minutes at room temperature.

After 5 washes in 0.5% Tween-PBS, the blots were incubated in 4000-fold diluted streptavidin-biotinylated horseradish peroxidase complex (Amersham Biosciences) for 30 minutes at room temperature. After 2 washes in Tween-PBS, bound antibodies were detected using the Western blotting Chemiluminescence Luminol Reagent (Santa Cruz Biotechnology, Santa Cruz, CA). The blots were then exposed on Hyperfilm ECL film (Amersham Biosciences).

Transfection and assay for cell proliferation

For the construction of vectors expressing *MEL1* and *MEL1S* genes, *MEL1* and *MEL1S* cDNA were subcloned into pME18Sneo (K. Maruyama and A. Miyajima, unpublished data, 2000), which was modified from pCEV4.[33] The mouse interleukin 2 (IL-2)–dependent T-cell line, CTLL-2, was maintained in RPMI 1640 supplemented with 10% fetal calf serum (FCS), 50 μM 2-mercaptoethanol, and 50 units/mL of human recombinant IL-2. Expression vectors and control vector were transfected into CTLL-2 cells by electroporation, and those cells were selected by G418 selection (0.75 mg/mL). Three transfectants, CTLL-2/pME18Sneo, CTLL-2/MEL1, and CTLL-2/MEL1S, were established. The expression of *MEL1* mRNA in cell clones was investigated by RT-PCR. For cell proliferation studies, MEL-expressing clones (CTLL-2/MEL1 and CTLL-2/MEL1S) and the control clone (CTLL-2/pME18Sneo) were plated at a density of 4×10^3 cells/well in 96-well microtiter plates. Cells were treated with increasing concentrations of transforming growth factor β (TGF-β; R&D Systems, Minneapolis, MN) for 96 hours and assayed for cell growth by the methyl thiazolyl tetrazolium (MTT) assay. Each experiment was performed 3 times, and typical results are shown.

Rapid amplification of cDNA 5′ ends (5′-RACE)

The 5′ terminus of *MEL1S* mRNA was determined by the SMART (Switching mechanism at the 5′ end of RNA transcript) RACE (rapid amplification of complementary DNA ends) cDNA Amplification Kit (BD Biosciences Clontech) according to the protocol provided by the manufacturer. The cDNA was synthesized by reverse transcription (PowerScript Reverse Transcriptase; BD Biosciences Clontech) of 1 μg of ATL-55T total RNA using 5′CDS primer (modified oligo [dT] primer) and SMARTIIA oligonucleotide. The first-strand cDNA was used directly in 5′-RACE PCR. For nested PCR amplifications, primers specific for the MEL1 gene (5′-CTCGGTGTGCACATGAAGAATACCGCG-3′ and 5′-AGGTCGAACCTGACCTTCTCAAGCAGT-3′) were used. The PCR products were subcloned into a TA cloning vector (pGEM-T Easy Vector; Promega) and sequenced.

Results

Identification of differentially hypomethylated CpG islands in ATL by MCA/RDA

To identify the differentially hypomethylated DNA regions in ATL, we used the MCA/RDA method. Genomic DNA extracted from peripheral blood mononuclear cells (PBMCs) of a carrier was used as a tester and that from acute ATL cells was used as a driver. After 2 rounds of RDA, the PCR products were cloned into plasmids and sequenced, resulting in identification of 16 DNA fragments. Thereafter, we checked that isolated DNA specifically hybridized to the tester amplicon by Southern blot analysis, in which MCA products were used as substrates as described in "Materials and methods." Specific hybridization to the tester amplicon implied that isolated DNAs were hypomethylated in ATL cells compared with PBMCs from a carrier. Finally, we identified 3 differentially hypomethylated DNA fragments in ATL cells as shown in Table 1. The *MEL1* (*MDS1/EVI1*-like gene 1) gene, which was mapped to human chromosome 1p36, was transcriptionally activated in acute myeloid leukemia or myelodysplastic syndrome with t(1;3)(p36;q21).[34] Another gene was *CACNA1H* (α1H T type Ca^{2+} channel), which is mapped to human chromosome 16p13.3, and was normally transcribed in kidney and heart.[35] The *Nogo receptor* gene is associated with inhibition of neurites by interaction with its ligand, and its expression was observed in neurons.[36]

DNA methylation of *MEL1*, *CACNA1H*, and *Nogo receptor* genes

To reveal the detailed DNA methylation status, we studied DNA methylation of *MEL1*, *CACNA1H*, and *Nogo receptor* genes by sequencing using sodium bisulfite–treated genomic DNAs. In the case of *MEL1*, a DNA fragment within exon 9 was isolated by MCA/RDA. Although the 5′ region of this DNA fragment was hypermethylated in normal PBMCs, the number of methylated CpG sites decreased in an ATL cell line, ATL-55T (Figure 1A), confirming that the MCA/RDA method isolated the differentially hypomethylated DNA regions. On the other hand, DNA methylation in the 3′ region showed no difference between normal PBMCs and ATL-55T. In *CACNA1H*, CpG sites in both the 5′ and 3′ regions were hypomethylated in ATL-55T cells compared with PBMCs (Figure 1B). In addition, the *Nogo receptor* gene was also undermethylated in ATL-55T (Figure 1C). Thus, these data confirmed that CpG sites in the isolated DNA regions were hypomethylated in ATL cells when compared with control PBMCs.

Expression of *MEL1*, *CACNA1H*, and *Nogo receptor* mRNAs in ATL cell lines

Since hypomethylation of the *MEL1*, *CACNA1H*, and *Nogo receptor* genes might be associated with their aberrant expression in ATL cells, we analyzed the transcription of these genes by RT-PCR. As shown in Figure 2, transcripts of the *MEL1* gene were detected in all HTLV-I–associated cell lines and another T-cell line (Kit225), although its expression was not detectable in PBMCs and activated T cells. Transcripts of the *CACNA1H* and *Nogo receptor* genes were also detected in some HTLV-I–associated T-cell lines or non–HTLV-I–associated T-cell lines. Thus, these results showed that the *MEL1*, *CACNA1H*, and *Nogo receptor* genes were aberrantly transcribed in ATL cells, suggesting a linkage between DNA hypomethylation and the aberrant transcription. Among them, *MEL1* gene was most frequently transcribed in ATL cells.

Table 1. Hypomethylated DNA clones isolated by MCA/RDA in ATL cells

Clone no.	Blast homology	Size, bp	Identities, %	GenBank accession no.
3	*CACNA1H* gene (intron 1)	640	99	AE006466
6	*MEL1* complete cds (exon 9)	428	100	AB078876
12	Upstream of homo sapiens similar to *Nogo receptor, reticulon 4 receptor* (LOC96184), mRNA	508	100	XM_015620

CACNA1H indicates voltage-dependent T-type Ca^{2+} channel; and MEL1, MDS1/EVI-like gene 1.

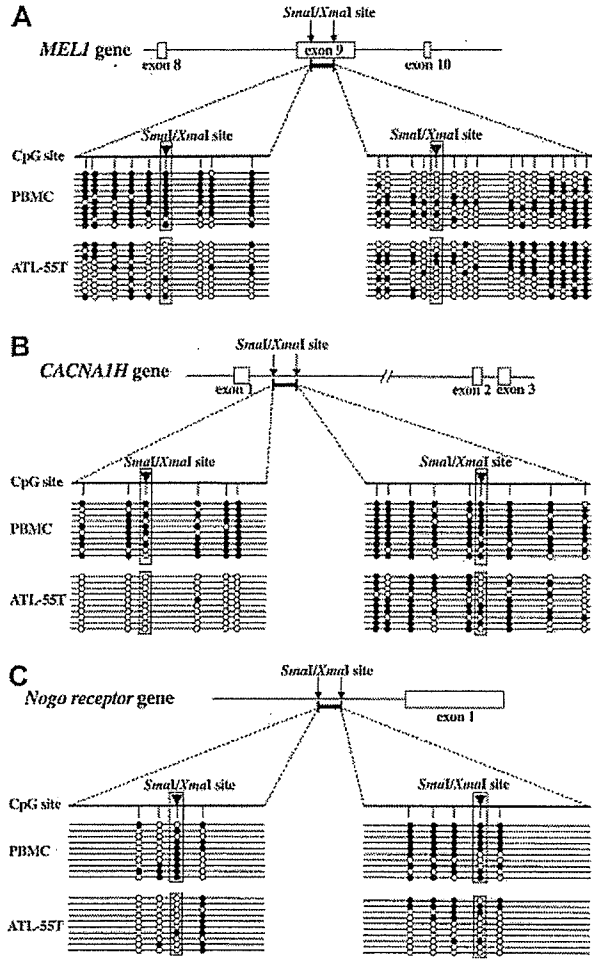

Figure 1. Methylation status of DNA fragments isolated by MCA/RDA. Genomic DNA was treated by sodium bisulfite and amplified by primers specific for DNA regions identified by MCA/RDA. Then, PCR products were subcloned into plasmid DNA, and the sequences were determined in 10 clones of each gene: (A) *MEL1*, (B) *CACNA1H*, and (C) *Nogo receptor* gene. The schemas show the structures of isolated DNA regions (bold bars), and arrowheads indicate the *SmaI/XmaI* sites. The methylation status of each CpG site is shown (●, methylated CpG; ○, unmethylated CpG).

Expression of *MEL1S* gene product in ATL cell lines

MEL1 is a member of the ecotropic viral integration site 1 (*EVI1*) gene family[34] and is also a PR (positive regulatory domain I binding factor 1 and retinoblastoma-interacting zinc finger protein) domain member (PRDM16).[37] Two forms of *MEL1* gene transcripts were identified, one encoded the full-length MEL1 protein with a PR domain and the other was the short form lacking PR domain (designated as MEL1S). *MEL1S*, but not *MEL1*, gene was expressed in t(1;3)(p36;q21)-positive myeloid leukemia cells by translocation, suggesting that MEL1S lacking the PR domain was associated with oncogenesis. To investigate which type of *MEL1* gene was expressed in ATL cells we analyzed *MEL1* and *MEL1S* gene expression by RT-PCR. As shown in Figure 3A, the 293 cell line expressed both types of *MEL1* gene transcripts; however, all ATL cell lines (MT-4, ATL-35T, ATL-43T, ATL-55T, ED, and ATL-2) predominantly expressed *MEL1S* type transcript. Moreover, we detected MEL1S protein in ATL-55T and ED, whereas the 293 cell line produced both MEL1 and 1S proteins by Western blot analysis (Figure 3B). Predominant expression of the *MEL1S* gene was also observed in Kit225 (data not shown). Taken together, these results showed that ATL cells produced MEL1S but not MEL1 protein.

Transcriptional initiation sites of the *MEL1S* gene have been determined in leukemic cells with t(1;3)(p36;q21), which showed that they existed in exon 2.[30] In acute myeloid leukemia cells with t(1;3)(p36;q21), translocation occurred in the promoter region or intron 1 of the *MEL1* gene and the *Ribophorin I* gene in 3q21, indicating that ectopic expression of *MEL1S* gene was driven by the *Ribophorin I* gene.[34,38] However, transcriptional initiation sites of the *MEL1S* gene in ATL cells remain unknown. Therefore, we determined the initiation sites of the *MEL1S* gene by 5′-RACE (Figure 4A) in ATL-55T. The 2 major PCR products observed in Figure 4A were cloned into plasmid DNA, and their sequences were determined. All 8 clones containing the upper band had a 633-bp sequence upstream from exon 6 (Figure 4B, number 1). On the other hand, among the 8 clones that contained the lower band, 6 contained a 410-bp sequence upstream from exon 6 (Figure 4B, number 2), and the remaining 2 clones started from 477-bp upstream of exon 4 and a putative exon (154 bp) spliced to exon 5 (Figure 4B, number 3). All transcripts lacked the PR domain, which was encoded by exons 2, 3, 4, and 5. Thus, 5′-RACE identified 3 different initiation sites of *MEL1S* gene transcription (Figure 4B). In other cell lines, ED and ATL-43T, the majority of transcripts of *MEL1S* initiated from the putative exon upstream exon 4 (Figure 4B, number 3). Therefore, this transcriptional initiation site is predominant for *MEL1S* gene transcription in ATL cells. We next

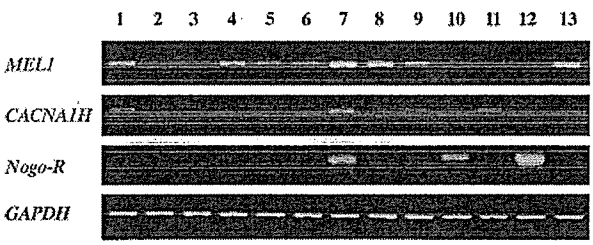

Figure 2. Expression of genes isolated by MCA/RDA in various cell lines. Expression of the *MEL1*, *CACNA1H*, and *Nogo receptor* genes, as identified by MCA/RDA, was analyzed by RT-PCR. Transcripts of the *GAPDH* gene were used as a control. Lane 1, 293 cells; lane 2, PBMCs; lane 3, activated T cells; lane 4, MT-4; lane 5, ATL-35T; lane 6, ATL-43T; lane 7, ATL-55T; lane 8, ED; lane 9, ATL-2; lane 10, Hut78; lane 11, Jurkat; lane 12, SupT1; and lane 13, Kit225.

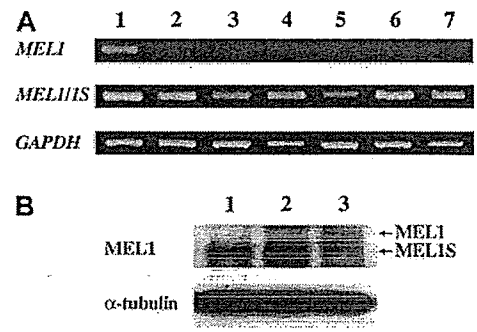

Figure 3. Short form products of the *MEL1* gene were expressed in ATL cell lines. (A) Transcription of *MEL1* and *MEL1S* genes. The transcription of *MEL1* and *MEL1S* genes were studied with the specific primers in ATL cell lines and control cell line as follows: lane 1, 293 cells; lane 2, MT-4; lane 3, ATL-35T; lane 4, ATL-43T; lane 5, ATL-55T; lane 6, ED; and lane 7, ATL-2. RT-PCR that could detect both *MEL1* and *MEL1S* gene transcripts revealed the transcription (330 bp) in all cell lines, whereas RT-PCR with primers specific for *MEL1* gene detected the transcript (197 bp) only in 293 cells. (B) Western blot analysis of MEL1 and MEL1S. Cell lysates were analyzed by Western blot using antibodies against the MEL1/1S protein. Lane 1, ATL-55T; lane 2, ED; and lane 3, 293 cells.

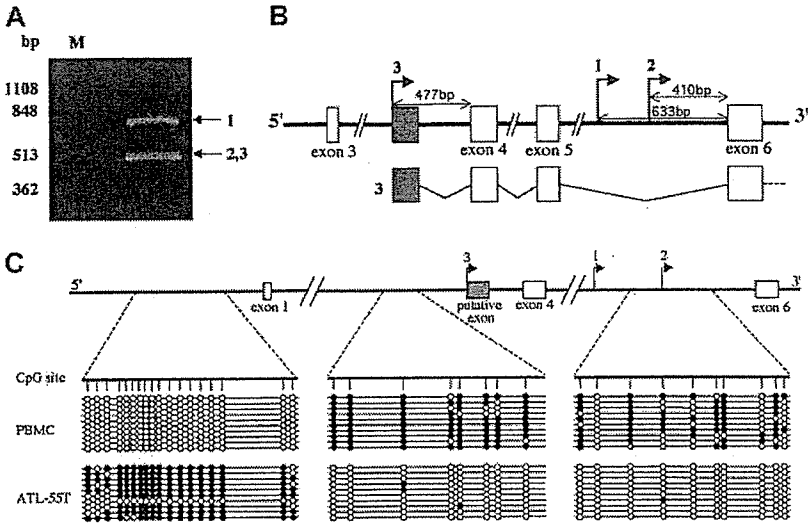

Figure 4. Identification of transcriptional initiation sites of the *MEL1S* gene, and DNA methylation. (A) The 5′-RACE was performed with cDNA synthesized using mRNA from an ATL cell line, ATL-55T. Primers in exon 6 were used to amplify cDNA. Two major bands were detected. (B) Schema of transcriptional initiation sites of the *MEL1S* gene in ATL cells. PCR products of 5′-RACE were cloned into plasmid DNA and then their sequences were determined. The majority of *MEL1S* transcripts initiated from upstream of exon 6 (633 bp [1] and 410 bp [2] upstream from exon 6 as shown in Figure 4B). Transcription started 477 bp upstream of the exon 4, which contained putative exon (▤; 154 bp [3]). From these data, 2 major initiation sites were identified as shown in 1 and 2. (C) The methylation status surrounding the transcriptional initiation sites of *MEL1S* gene and promoter region of *MEL1* gene. Genomic DNA was treated by sodium bisulfite and amplified by specific primers. The methylation status was determined by sequencing of these PCR products. The schema shows the structure of the *MEL1/1S* gene and transcriptional initiation sites of the *MEL1S* gene are shown by arrows (1, 2, and as described for panel B). Methylation of CpG sites surrounding the transcriptional initiation sites of *MEL1S* is shown (●, methylated; ○, unmethylated).

determined the methylation status of DNA regions surrounding these initiation sites (Figure 4C). As observed in the coding region of the *MEL1* gene (Figure 1A), these regions surrounding the transcriptional initiation sites were also hypomethylated in ATL cells compared with normal PBMCs, suggesting that aberrant expression of the *MEL1S* gene was associated with hypomethylation in the putative promoter region of the *MEL1S* gene. In contrast to the *MEL1S* gene, the promoter region of *MEL1* was not methylated in PBMCs but was hypermethylated in ATL-55T (Figure 4C), showing that in contrast to the *MEL1S* gene, transcription of *MEL1* was silenced in ATL cells by DNA hypermethylation.

MEL expression conferred resistance against TGF-β

The *EVI1* gene is an alternative splicing form of the *MDS1/EVI* gene; MDS1/EVI1 retains PR domain whereas EV1 lacks it. EVI1 has been reported to repress the growth suppression mediated by TGF-β against a mouse IL-3–dependent myeloid cell line, 32Dcl3, whereas MDS1/EVI1 enhanced TGF-β signaling and strengthened its growth-inhibitory effect.[39] Structural similarity between MEL1S and EVI1 suggested that MEL1S might be associated with the growth inhibitory effect of TGF-β. ATL cell lines expressing MEL1S were resistant to TGF-β, whereas mouse T-cell line, CTLL-2, was sensitive to it (Figure 5A). To determine whether MEL could influence the antiproliferative effects of TGF-β, we established CTLL-2 cell lines stably expressing MEL1 and MEL1S by transfection of the respective expression vectors. RT-PCR confirmed their expressions (Figure 5B). TGF-β suppressed the growth of a CTLL-2 cell line in a dose-dependent manner. Although CTLL-2/MEL1 cells showed increased susceptibility to TGF-β, CTLL-2/MEL1S cells exhibited resistance against TGF-β (Figure 5C). These results showed that MEL1 protein with the PR domain and MEL1S protein without the PR domain had differential influences on susceptibility to TGF-β responsiveness and that MEL1S protein lacking the PR domain rendered ATL cells resistant to the inhibitory effect of TGF-β as well as EVI1.

Discussion

Hypomethylation has been demonstrated to be associated with genetic instability and aberrant gene expression.[14] Most hypomethylated genes have been identified by analyses of known genes, such as oncogenes[29] and genes associated with drug resistance.[28] However, several different methods have been applied for isolation

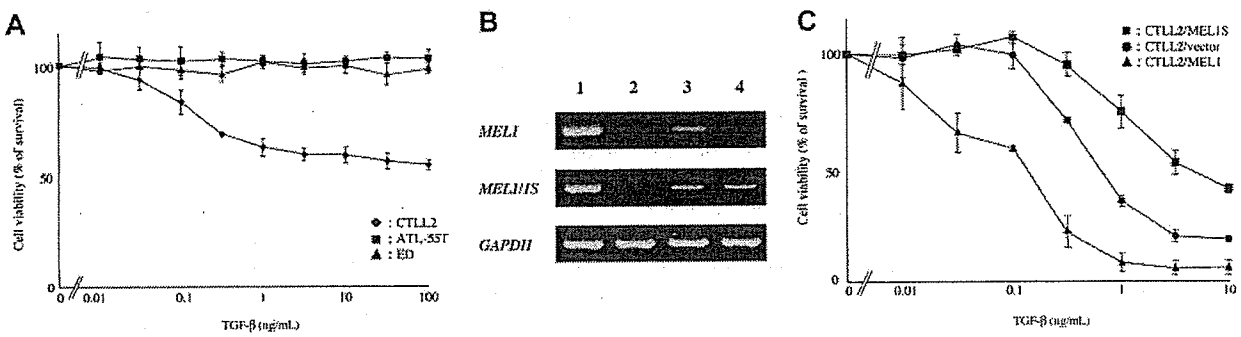

Figure 5. Sensitivity to TGF-β in ATL cell lines and CTLL-2 cell lines expressing *MEL1* or *MEL1S* gene. (A) Resistance of ATL cell lines to TGF-β. ATL cell lines, ATL-55T and ED, and mouse T-cell line, CTLL-2, were treated with the indicated concentrations of TGF-β for 72 hours. Proliferation of each cell was examined by MTT assay. The results are shown as percentages of the values obtained from control TGF-β–free culture. The experiment was performed at least 3 times. The results are the mean ± SD of 3 experiments. (B) Expression of *MEL1* and *MEL1S* gene in CTLL-2 transfected with vectors expressing *MEL1* or *MEL1S* genes. CTLL-2 was transfected with vectors expressing *MEL1* or *MEL1S* genes, and their expressions were studied by RT-PCR as described in Figure 3. Lane 1 shows 293 cells (control); lane 2, CTLL-2/empty vector; lane 3, CTLL-2/MEL1; and lane 4, CTLL-2/MEL1S. (C) MEL1S expression confers resistance against TGF-β in CTLL-2. MEL1-expressing (▲, MEL1; ■, MEL1S) and unmodified (●) CTLL-2 were treated with the indicated concentrations of TGF-β for 96 hours. The results are shown as percentages of the values obtained from control TGF-β–free culture. The results are the mean ± SD of 3 experiments.

of aberrantly methylated DNA regions, which include restriction landmark genomic screening (RLGS)[40] and methylation-sensitive–representational difference analysis (MS-RDA),[41] in addition to MCA/RDA.[31] For isolation of hypomethylated DNA regions, the RLGS method revealed that the peri-centromeric region of human acrochromosomes was hypomethylated in hepatitis B virus (HBV)–integrated hepatocellular carcinoma (HCC) cells.[42] It has also been shown that a 1.4-kb repetitive sequence was hypomethylated in sperm and HCC cells.[43] MS-RDA could also detect hypomethylated DNA regions in mouse HCC, which included the long interspersed nuclear element 1 (LINE-1) and α-enolase genes.[41] In addition to these methods, MCA/RDA also identified hypomethylated DNA regions as shown in the present study. Among the 3 hypomethylated genes identified in the present study, the *CACNA1H* and *Nogo receptor* genes were not as frequently expressed in ATL cells, although their expression was associated with hypomethylation. On the other hand, the *MEL1S* gene was aberrantly expressed in ATL cells and also exhibited hypomethylation in ATL cells compared with PBMCs. Thus, the MCA/RDA method could isolate hypomethylated DNA regions in addition to hypermethylated DNA regions, as reported previously.[31] Although repetitive sequences are hypomethylated in cancer cells, MCA/RDA could not isolate these sequences in this study. Since MCA/RDA detected differentially methylated *SmaI*/*XmaI* sites, the rarity of such sites in the repetitive sequences might account for the inability of MCA/RDA to isolate the repetitive sequences. DNA methylation of promoter regions influences transcription in general, and the DNA regions isolated by MCA/RDA method were not the promoter regions of the *MEL1S* and *CACNA1H* genes. However, hypomethylation in the nonpromoter DNA regions was linked with aberrant expression of these genes. Indeed, the putative promoter region of the *MEL1S* gene was also hypomethylated in ATL cells as shown in our study, indicating that hypomethylation of nonpromoter regions was associated with aberrant transcription and hypomethylation of promoter regions.

The *MEL1* gene, which was mapped to human chromosome 1p36, was originally isolated as the gene that was transcriptionally activated by t(1;3)(p36;q21) in acute myeloid leukemia.[34] This gene encodes 2 types of transcripts, *MEL1* and *MEL1S*. The *MEL1* gene that retains the PR domain is highly homologous to *MDS1/EVI1*, whereas the *MEL1S* gene is an alternatively spliced transcript of *MEL1* gene, which lacks the PR domain as observed in *EVI1*. In 293 cells, both *MEL1* and *MEL1S* genes were transcribed, although only *MEL1S* gene transcripts were detected in AML cells with t(1;3)(p36;q21). Another PR domain–containing gene, *RIZ* (the retinoblastoma protein-interacting zinc finger gene) was identified,[44] which also encodes 2 types of transcripts, a PR-positive and PR-negative form. In the *MDS1/EVI1*, *MEL1*, and *RIZ* genes, transcripts lacking the PR domain have all been associated with oncogenesis as observed in the present study. The *EVI1* gene that lacked the PR domain was transcribed in leukemic cells by retroviral integration[45] or translocation.[46,47] The expression of *RIZ1* (PR domain positive) was suppressed by DNA hypermethylation,[48] whereas expression of *RIZ2* (PR domain negative) gene was intact in colorectal cancer[49] and breast cancer cells,[50] resulting in predominant expression of the PR domain–negative form. Moreover, inactivation of the *RIZ1* gene allowed tumor formation in vivo.[51] Taken together, these findings indicate that the PR domain had a tumor-suppressive character, whereas transcripts without the PR domain were oncogenic. In normal tissues, transcripts both with and without the PR domain were observed.[50,52] In *MEL1* gene, the pattern of DNA methylation of *MEL1* and *MEL1S* gene promoter regions is contrast between ATL cells and PBMCs. Since both genes are not transcribed in PBMCs and activated T cells, lack of transcriptional factors necessary for *MEL1* and *MEL1S* genes transcription or the presence of silencer is considered the cause of an absence of transcription, since the *MEL1* promoter is hypomethylated regardless of lack of *MEL1* gene expression. In the fetal kidney, both *MEL1* and *MEL1S* genes are transcribed, suggesting that common transcriptional machinery is involved in their transcriptions. On the other hand, DNA hypermethylation in the promoter region of *MEL1* gene associated with DNA hypomethylation in that of *MEL1S* gene alters the expression pattern of *MEL1/MEL1S* gene in ATL cells, as observed in *RIZ1/RIZ2* genes.

Predominant expression of the PR domain–negative form by retroviral insertion, translocation, hypermethylation, and hypomethylation (this study) was linked to oncogenesis. Increased expression of the *MEL1S* gene with suppressed expression of the PR domain–positive form is considered to facilitate proliferation of leukemic cells. One mechanism by which PR domain–negative forms might be associated with oncogenesis is that the PR domain–negative form of both *EVI1* and *MEL1S* genes inhibits the tumor-suppressive effect of TGF-β. However, the findings that both EVI1 and MEL1S could inhibit the differentiation of myeloid cells[30] suggested another mechanism in the oncogenesis of ATL.

The PR domain is composed of about 130 amino acid residues and shares significant sequence identity to the SET domain. This domain is present in suppressor of variegation 3-9 homolog 1 (SUV39H1),[53] SET1 (yeast),[54] and human trithorax,[55] which are contained in chromosomal proteins that function in modulating gene expression. Recent studies have identified the suppressor of variegation 3-9 family as being H3 lysine 9–specific histone methyltransferase.[53] These proteins, which play an important role in the establishment and maintenance of heterochromatin, mediate their methylation activities via the SET domain. The finding that the shared residues between PR and SET are contained in the most conserved residues in each domain indicates that they might share a common function.[56] The tumor-suppressive effects shared by all PR domain–containing genes suggested that they influenced the function of PR domain–negative forms, such as MEL1S and EVI1, by acting on chromatin structures. The mechanism(s) by which PR domain–negative forms, such as MEL1S and EVI1, are associated with oncogenesis remains to be elucidated.

The *EVI1* gene (PR domain negative) is an alterative splicing form of *MDS1/EVI1* gene (PR domain positive). It has been reported that EVI1 represses TGF-β signaling through inhibition of Smad3,[57] however, MDS1/EVI1 enhanced TGF-β signaling and strengthened its growth-inhibitory effect.[39] Consequently, the inappropriate expression of the PR-negative oncogenic product, EVI1, in hematopoietic cells has been implicated in the oncogenesis of acute myeloid leukemia. In this study, we also reported that MEL1S, lacking the PR domain, conferred resistance against TGF-β, whereas MEL1 increased susceptibility to TGF-β. In HTLV-I–infected cells, the expression of Tax conferred resistance against TGF-β, as reported previously.[58-60] However, Tax protein could not be produced by genetic changes of the HTLV-I provirus genome in most fresh ATL cells, suggesting an alternative mechanism for resistance against TGF-β.[61,62] Although the ATL cell lines ATL-55T, 43T, and ED could not produce Tax protein due to mutation or deletion of the *tax* gene and hypermethylation of the 5′-LTR,[63] they secreted TGF-β and were resistant to it (Figure 5A). The *MEL1S* gene was transcribed in Tax-negative ATL cells, such as ATL-43T, ED, and ATL-55T, suggesting that MEL1S rendered ATL cells resistant to TGF-β in the absence of Tax.

The *CACNA1H* (α1H T type Ca^{2+} channel) gene was also identified as a hypomethylated gene in ATL cells, although the frequency of aberrant expression was not as high (2 of 6 ATL cell lines). It has been reported that antagonists of T-type Ca^{2+} channels (CACNA1H) inhibited cell proliferation,[64] suggesting that its aberrant expression is associated with cell proliferation.

In conclusion, we have demonstrated in the present study that MCA/RDA is a powerful method for identifying hypomethylated and aberrantly transcribed genes in cancer cells. Identification of aberrantly expressed genes associated with hypomethylation should help elucidate mechanisms of oncogenesis.

Acknowledgments

We are grateful to Ei-ichi Kodama and Yoshihiro Koya for valuable suggestions. The authors also thank Dr F. G. Issa (wordmedex.com.au) for the careful reading and editing of the manuscript.

References

1. Takatsuki K, Uchiyama T, Sagawa K, Yodoi J. Adult T cell leukemia in Japan. In: Seno S, Takaku F, Irino S, eds. Topics in Hematology, the 16th International Congress of Hematology. Amsterdam, The Netherlands: Excerpta Medica; 1977:73-77.
2. Uchiyama T, Yodoi J, Sagawa K, Takatsuki K, Uchino H. Adult T-cell leukemia: clinical and hematologic features of 16 cases. Blood. 1977;50: 481-492.
3. Poiesz BJ, Ruscetti FW, Gazdar AF, Bunn PA, Minna JD, Gallo RC. Detection and isolation of type C retrovirus particles from fresh and cultured lymphocytes of a patient with cutaneous T-cell lymphoma. Proc Natl Acad Sci U S A. 1980;77: 7415-7419.
4. Hinuma Y, Nagata K, Hanaoka M, et al. Adult T-cell leukemia: antigen in an ATL cell line and detection of antibodies to the antigen in human sera. Proc Natl Acad Sci U S A. 1981;78:6476-6480.
5. Yoshida M, Miyoshi I, Hinuma Y. Isolation and characterization of retrovirus from cell lines of human adult T-cell leukemia and its implication in the disease. Proc Natl Acad Sci U S A. 1982;79: 2031-2035.
6. Wong-Staal F, Gallo RC. Human T-lymphotropic retroviruses. Nature. 1985;317:395-403.
7. Franchini G. Molecular mechanisms of human T-cell leukemia/lymphotropic virus type I infection. Blood. 1995;86:3619-3639.
8. Yoshida M. Multiple viral strategies of htlv-1 for dysregulation of cell growth control. Annu Rev Immunol. 2001;19:475-496.
9. Neuveut C, Jeang KT. Cell cycle dysregulation by HTLV-I: role of the tax oncoprotein. Front Biosci. 2002;7:d157-d163.
10. Arisawa K, Soda M, Endo S, et al. Evaluation of adult T-cell leukemia/lymphoma incidence and its impact on non-Hodgkin lymphoma incidence in southwestern Japan. Int J Cancer. 2000;85:319-324.
11. Sakashita A, Hattori T, Miller CW, et al. Mutations of the p53 gene in adult T-cell leukemia. Blood. 1992;79:477-480.
12. Hatta Y, Hirama T, Miller CW, Yamada Y, Tomonaga M, Koeffler HP. Homozygous deletions of the p15 (MTS2) and p16 (CDKN2/MTS1) genes in adult T-cell leukemia. Blood. 1995;85: 2699-2704.
13. Nosaka K, Maeda M, Tamiya S, Sakai T, Mitsuya H, Matsuoka M. Increasing methylation of the CDKN2A gene is associated with the progression of adult T-cell leukemia. Cancer Res. 2000;60: 1043-1048.
14. Ehrlich M. DNA methylation in cancer: too much, but also too little. Oncogene. 2002;21:5400-5413.
15. Santini V, Kantarjian HM, Issa JP. Changes in DNA methylation in neoplasia: pathophysiology and therapeutic implications. Ann Intern Med. 2001;134:573-586.
16. Herman JG, Merlo A, Mao L, et al. Inactivation of the CDKN2/p16/MTS1 gene is frequently associated with aberrant DNA methylation in all common human cancers. Cancer Res. 1995;55:4525-4530.
17. Herman JG, Jen J, Merlo A, Baylin SB. Hypermethylation-associated inactivation indicates a tumor suppressor role for p15INK4B. Cancer Res. 1996;56:722-727.
18. Kane MF, Loda M, Gaida GM, et al. Methylation of the hMLH1 promoter correlates with lack of expression of hMLH1 in sporadic colon tumors and mismatch repair-defective human tumor cell lines. Cancer Res. 1997;57:808-811.
19. Dobrovic A, Simpfendorfer D. Methylation of the BRCA1 gene in sporadic breast cancer. Cancer Res. 1997;57:3347-3350.
20. Lee WH, Morton RA, Epstein JI, et al. Cytidine methylation of regulatory sequences near the pi-class glutathione S-transferase gene accompanies human prostatic carcinogenesis. Proc Natl Acad Sci U S A. 1994;91:11733-11737.
21. Feinberg AP, Vogelstein B. Hypomethylation distinguishes genes of some human cancers from their normal counterparts. Nature. 1983;301:89-92.
22. Gama-Sosa MA, Slagel VA, Trewyn RW, et al. The 5-methylcytosine content of DNA from human tumors. Nucleic Acids Res. 1983;11:6883-6894.
23. Goelz SE, Vogelstein B, Hamilton SR, Feinberg AP. Hypomethylation of DNA from benign and malignant human colon neoplasms. Science. 1985;228:187-190.
24. Gaudet F, Hodgson JG, Eden A, et al. Induction of tumors in mice by genomic hypomethylation. Science. 2003;300:489-492.
25. Okano M, Bell DW, Haber DA, Li E. DNA methyltransferases Dnmt3a and Dnmt3b are essential for de novo methylation and mammalian development. Cell. 1999;99:247-257.
26. Xu GL, Bestor TH, Bourc'his D, et al. Chromosome instability and immunodeficiency syndrome caused by mutations in a DNA methyltransferase gene. Nature. 1999;402:187-191.
27. De Smet C, De Backer O, Faraoni I, Lurquin C, Brasseur F, Boon T. The activation of human gene MAGE-1 in tumor cells is correlated with genome-wide demethylation. Proc Natl Acad Sci U S A. 1996;93:7149-7153.
28. Nakayama M, Wada M, Harada T, et al. Hypomethylation status of CpG sites at the promoter region and overexpression of the human MDR1 gene in acute myeloid leukemias. Blood. 1998; 92:4296-4307.
29. Watt PM, Kumar R, Kees UR. Promoter demethylation accompanies reactivation of the HOX11 proto-oncogene in leukemia. Genes Chromosomes Cancer. 2000;29:371-377.
30. Nishikata I, Sasaki H, Iga M, et al. A novel EVI1 gene family, MEL1 lacking a PR domain (MEL1S) is mainly expressed in t(1;3)(p36;q21)-positive AML and blocks G-CSF-induced myeloid differentiation. Blood. 2003;102:3323-3332.
31. Toyota M, Ho C, Ahuja N, et al. Identification of differentially methylated sequences in colorectal cancer by methylated CpG island amplification. Cancer Res. 1999;59:2307-2312.
32. Nosaka K, Miyamoto T, Sakai T, Mitsuya H, Suda T, Matsuoka M. Mechanism of hypercalcemia in adult T-cell leukemia: overexpression of receptor activator of nuclear factor kappaB ligand on adult T-cell leukemia cells. Blood. 2002;99:634-640.
33. Itoh N, Yonehara S, Schreurs J, et al. Cloning of an interleukin-3 receptor gene: a member of a distinct receptor gene family. Science. 1990;247: 324-327.
34. Mochizuki N, Shimizu S, Nagasawa T, et al. A novel gene, MEL1, mapped to 1p36.3 is highly homologous to the MDS1/EVI1 gene and is transcriptionally activated in t(1;3)(p36;q21)-positive leukemia cells. Blood. 2000;96:3209-3214.
35. Cribbs LL, Lee JH, Yang J, et al. Cloning and characterization of alpha1H from human heart, a member of the T-type Ca2+ channel gene family. Circ Res. 1998;83:103-109.
36. Wang KC, Koprivica V, Kim JA, et al. Oligodendrocyte-myelin glycoprotein is a Nogo receptor ligand that inhibits neurite outgrowth. Nature. 2002;417:941-944.
37. Jiang GL, Huang S. The yin-yang of PR-domain family genes in tumorigenesis. Histol Histopathol. 2000;15:109-117.
38. Xinh PT, Tri NK, Nagao H, et al. Breakpoints at 1p36.3 in three MDS/AML(M4) patients with t(1; 3)(p36;q21) occur in the first intron and in the 5' region of MEL1. Genes Chromosomes Cancer. 2003;36:313-316.
39. Sood R, Talwar-Trikha A, Chakrabarti SR, Nucifora G. MDS1/EVI1 enhances TGF-beta1 signaling and strengthens its growth-inhibitory effect but the leukemia-associated fusion protein AML1/MDS1/EVI1, product of the t(3;21), abrogates growth-inhibition in response to TGF-beta1. Leukemia. 1999;13:348-357.
40. Hayashizaki Y, Hirotsune S, Okazaki Y, et al. Restriction landmark genomic scanning method and its various applications. Electrophoresis. 1993;14: 251-258.
41. Ushijima T, Morimura K, Hosoya Y, et al. Establishment of methylation-sensitive-representational difference analysis and isolation of hypo- and hypermethylated genomic fragments in mouse liver tumors. Proc Natl Acad Sci U S A. 1997;94:2284-2289.
42. Nagai H, Baba M, Konishi N, et al. Isolation of NotI clusters hypomethylated in HBV-integrated hepatocellular carcinomas by two-dimensional electrophoresis. DNA Res. 1999;6:219-225.
43. Nagai H, Kim YS, Yasuda T, et al. A novel sperm-specific hypomethylation sequence is a demethylation hotspot in human hepatocellular carcinomas. Gene. 1999;237:15-20.
44. Buyse IM, Shao G, Huang S. The retinoblastoma protein binds to RIZ, a zinc-finger protein that shares an epitope with the adenovirus E1A protein. Proc Natl Acad Sci U S A. 1995;92:4467-4471.
45. Morishita K, Parker DS, Mucenski ML, Jenkins NA, Copeland NG, Ihle JN. Retroviral activation of a novel gene encoding a zinc finger protein in IL-3-dependent myeloid leukemia cell lines. Cell. 1988;54:831-840.
46. Morishita K, Parganas E, William CL, et al. Activation of EVI1 gene expression in human acute myelogenous leukemias by translocations spanning 300-400 kilobases on chromosome band

3q26. Proc Natl Acad Sci U S A. 1992;89:3937-3941.

47. Nucifora G, Begy CR, Kobayashi H, et al. Consistent intergenic splicing and production of multiple transcripts between AML1 at 21q22 and unrelated genes at 3q26 in (3;21)(q26;q22) translocations. Proc Natl Acad Sci U S A. 1994;91:4004-4008.
48. Du Y, Carling T, Fang W, Piao Z, Sheu JC, Huang S. Hypermethylation in human cancers of the RIZ1 tumor suppressor gene, a member of a histone/protein methyltransferase superfamily. Cancer Res. 2001;61:8094-8099.
49. Chadwick RB, Jiang GL, Bennington GA, et al. Candidate tumor suppressor RIZ is frequently involved in colorectal carcinogenesis. Proc Natl Acad Sci U S A. 2000;97:2662-2667.
50. He L, Yu JX, Liu L, et al. RIZ1, but not the alternative RIZ2 product of the same gene, is underexpressed in breast cancer, and forced RIZ1 expression causes G2-M cell cycle arrest and/or apoptosis. Cancer Res. 1998;58:4238-4244.
51. Steele-Perkins G, Fang W, Yang XH, et al. Tumor formation and inactivation of RIZ1, an Rb-binding member of a nuclear protein-methyltransferase superfamily. Genes Dev. 2001;15:2250-2262.
52. Fears S, Mathieu C, Zeleznik-Le N, Huang S, Rowley JD, Nucifora G. Intergenic splicing of MDS1 and EVI1 occurs in normal tissues as well as in myeloid leukemia and produces a new member of the PR domain family. Proc Natl Acad Sci U S A. 1996;93:1642-1647.
53. Rea S, Eisenhaber F, O'Carroll D, et al. Regulation of chromatin structure by site-specific histone H3 methyltransferases. Nature. 2000;406:593-599.
54. Nislow C, Ray E, Pillus L. SET1, a yeast member of the trithorax family, functions in transcriptional silencing and diverse cellular processes. Mol Biol Cell. 1997;8:2421-2436.
55. Nakamura T, Mori T, Tada S, et al. ALL-1 is a histone methyltransferase that assembles a supercomplex of proteins involved in transcriptional regulation. Mol Cell. 2002;10:1119-1128.
56. Huang S, Shao G, Liu L. The PR domain of the Rb-binding zinc finger protein RIZ1 is a protein binding interface and is related to the SET domain functioning in chromatin-mediated gene expression. J Biol Chem. 1998;273:15933-15939.
57. Kurokawa M, Mitani K, Irie K, et al. The oncoprotein Evi-1 represses TGF-beta signalling by inhibiting Smad3. Nature. 1998;394:92-96.
58. Mori N, Morishita M, Tsukazaki T, et al. Human T-cell leukemia virus type I oncoprotein Tax represses Smad-dependent transforming growth factor beta signaling through interaction with CREB-binding protein/p300. Blood. 2001;97:2137-2144.
59. Arnulf B, Villemain A, Nicot C, et al. Human T-cell lymphotropic virus oncoprotein Tax represses TGF-beta 1 signaling in human T cells via c-Jun activation: a potential mechanism of HTLV-I leukemogenesis. Blood. 2002;100:4129-4138.
60. Lee DK, Kim BC, Brady JN, Jeang KT, Kim SJ. Human T-cell lymphotropic virus type 1 tax inhibits transforming growth factor-beta signaling by blocking the association of Smad proteins with Smad-binding element. J Biol Chem. 2002;277:33766-33775.
61. Tamiya S, Matsuoka M, Etoh K, et al. Two types of defective human T-lymphotropic virus type I provirus in adult T-cell leukemia. Blood. 1996;88:3065-3073.
62. Furukawa Y, Kubota R, Tara M, Izumo S, Osame M. Existence of escape mutant in HTLV-I tax during the development of adult T-cell leukemia. Blood. 2001;97:987-993.
63. Takeda S, Maeda M, Morikawa S, et al. Genetic and epigenetic inactivation of tax gene in adult T-cell leukemia cells. Int J Cancer. In press.
64. Bertolesi GE, Shi C, Elbaum L, et al. The Ca(2+) channel antagonists mibefradil and pimozide inhibit cell growth via different cytotoxic mechanisms. Mol Pharmacol. 2002;62:210-219.

Int. J. Cancer: **110**, 621–625 (2004)

Publication of the International Union Against Cancer

LETTER TO THE EDITOR

Role of HTLV-1 Proviral DNA Load and Clonality in the Development of Adult T-Cell Leukemia/Lymphoma in Asymptomatic Carriers

Akihiko OKAYAMA[1]*, Sherri STUVER[2,3], Masao MATSUOKA[4], Junzo ISHIZAKI[1], Gen-ichi TANAKA[1], Yoko KUBUKI[1], Nancy MUELLER[3], Chung-cheng HSIEH[5], Nobuyoshi TACHIBANA[6] and Hirohito TSUBOUCHI[1]

[1]*Department of Internal Medicine II, Miyazaki Medical College, Miyazaki, Japan*
[2]*Department of Epidemiology, Boston University School of Public Health, Boston, MA, USA*
[3]*Department of Epidemiology, Harvard School of Public Health, Boston, MA, USA*
[4]*Laboratory of Virus Immunology, Institute for Virus Research, Kyoto University, Kyoto, Japan*
[5]*Division of Biostatistics and Epidemiology, University of Massachusetts Medical School Cancer Center, Boston, MA, USA*
[6]*Department of Nursing Science, Miyazaki Prefectural Nursing College, Miyazaki, Japan*

Dear Sir,

Human T-lymphotropic virus type 1 (HTLV-1) is the causative agent for adult T-cell leukemia/lymphoma (ATL).[1–3] Only a small proportion of HTLV-1 carriers eventually develop ATL after a long latency.[4] However, the critical events in the leukemogenic process remain unclear. In general, viral load is an important factor affecting the outcome of virus-associated disease. The HTLV-1 proviral DNA load in the peripheral blood mononuclear cells (PBMCs) of carriers exhibits a wide range of values.[5] Enhanced expression of HTLV-1 Tax, which transactivates transcription of viral mRNA and of host genes that control cell proliferation, induces amplification of infected cells (*i.e.*, the number of proviral copies).[6] One of the host genes encodes the IL-2 receptor (IL-2R), which is overexpressed on the surface of ATL cells.[7] We have observed that subjects with detectable *tax/rex* mRNA have a higher number of IL-2Rα-positive T cells.[8] We also have found a positive association between HTLV-1 proviral load and the level of soluble IL-2R in asymptomatic carriers,[5] as well as the number of morphologically abnormal lymphocytes on a peripheral blood smear among carriers.[9,10] In addition, the HTLV-1 proviral load within a carrier is stable over many years.[5] It has been postulated that clonal proliferation of HTLV-1-infected cells likely is responsible for maintaining the proviral load level in a carrier.[11,12] HTLV-1 Tax may contribute to the clonal proliferation of HTLV-1-infected cells by promoting their abnormal growth.[6] Tax also exerts dysregulation of the cell cycle by binding to its inhibitors and inhibiting some tumor-suppressor proteins.[6]

The accumulated data support the hypothesis that increased HTLV-1 proviral load and clonal expansion of HTLV-1-infected cells are key to the process of leukemogenesis in HTLV-1 carriers. However, proviral DNA levels and clonality of HTLV-1-infected cells have not been directly evaluated as predictors of the development of ATL in asymptomatic carriers. Given an ATL incidence rate as low as 1 case per 1,000 person-years among HTLV-1 carriers, such a study would require extensive follow-up of a relatively large number of HTLV-1 carriers.

The Miyazaki Cohort Study is a population-based prospective study of the natural history of HTLV-1, which was established in 1984.[13] During follow-up of the cohort through December 2000, 6 ATL cases were identified through an annual census or reports from next-of-kin.[14] Four of the 6 cases had available prediagnostic samples of PBMCs and were included in the present analysis (Table I). Diagnosis was confirmed by medical records for 3 of the 4 cases (cases 1, 3, 4). Lymph node biopsy for case 4 and the PBMCs at ATL diagnosis for cases 1 and 4 were available for analysis. Any symptoms suggestive of smoldering- or chronic-type ATL, such as skin lesions or lymphadenopathy, were not observed at the annual health examinations prior to the diagnosis of malignancy in the cases studied. Routine blood tests performed at the annual health examinations also did not reveal any abnormal findings suggestive of subclinical ATL. Therefore, it is unlikely that these cases had smoldering- or chronic-type ATL before the onset of acute- or lymphoma-type ATL. For comparison of HTLV-1 proviral load, age- and sex-matched HTLV-1$^+$ controls were randomly selected from asymptomatic carriers within the cohort. Informed consent was obtained from all study participants, and the study protocol was approved by the Human Subjects Committees of Miyazaki Medical College and Harvard School of Public Health.

HTLV-1 proviral DNA in PBMCs was quantitated using the AmpliSensor assay (AcuGen HTLV-1 Quantitation Test; Biotronics, Lowell, MA).[5,15] Prediagnostic HTLV-1 proviral loads of the 4 ATL cases are shown in Table I. Two cases were male (cases 1, 2), and 2 were female (cases 3, 4). Median age at onset of ATL was 73.5 years (range 64–83). Median HTLV-1 proviral load (copies per 100,000 PBMCs) at the earliest prediagnostic PBMC sample (collected 3–8 years prior to ATL onset) was 4,930 (range 830–10,560). Median proviral

Grant sponsor: National Institutes of Health; Grant number: CA38450; Grant sponsor: Ministry of Education, Science, Sports and Culture (Japan).

*Correspondence to: Department of Internal Medicine II, Miyazaki Medical College, 5200 Kihara, Kiyotake, Miyazaki 8891601, Japan. Fax: +81-985-85-5194. E-mail: okayama@post1.miyazaki-med.ac.jp

Received 16 September 2003; Revised 17 December 2003; Accepted 7 January 2004

DOI 10.1002/ijc.20144
Published online 15 March 2004 in Wiley InterScience (www.interscience.wiley.com).

TABLE I – HTLV-1 PROVIRAL DNA LOADS IN 4 CARRIERS WHO EVENTUALLY DEVELOPED ATL

	Case 1	Case 2	Case 3	Case 4
Year before onset				
8				6,690[1]
7			830	
6				
5	3,170		1,910	2,200
4			1,480	
3		10,560		
2			2,110	18,150
1			2,840	
ATL type at diagnosis	Acute	Not available	Lymphoma	Lymphoma
Age[2] (years), sex	83, male	64, male	76, female	70, female

[1]Copies per 100,000 PBMCs.–[2]Age at death.

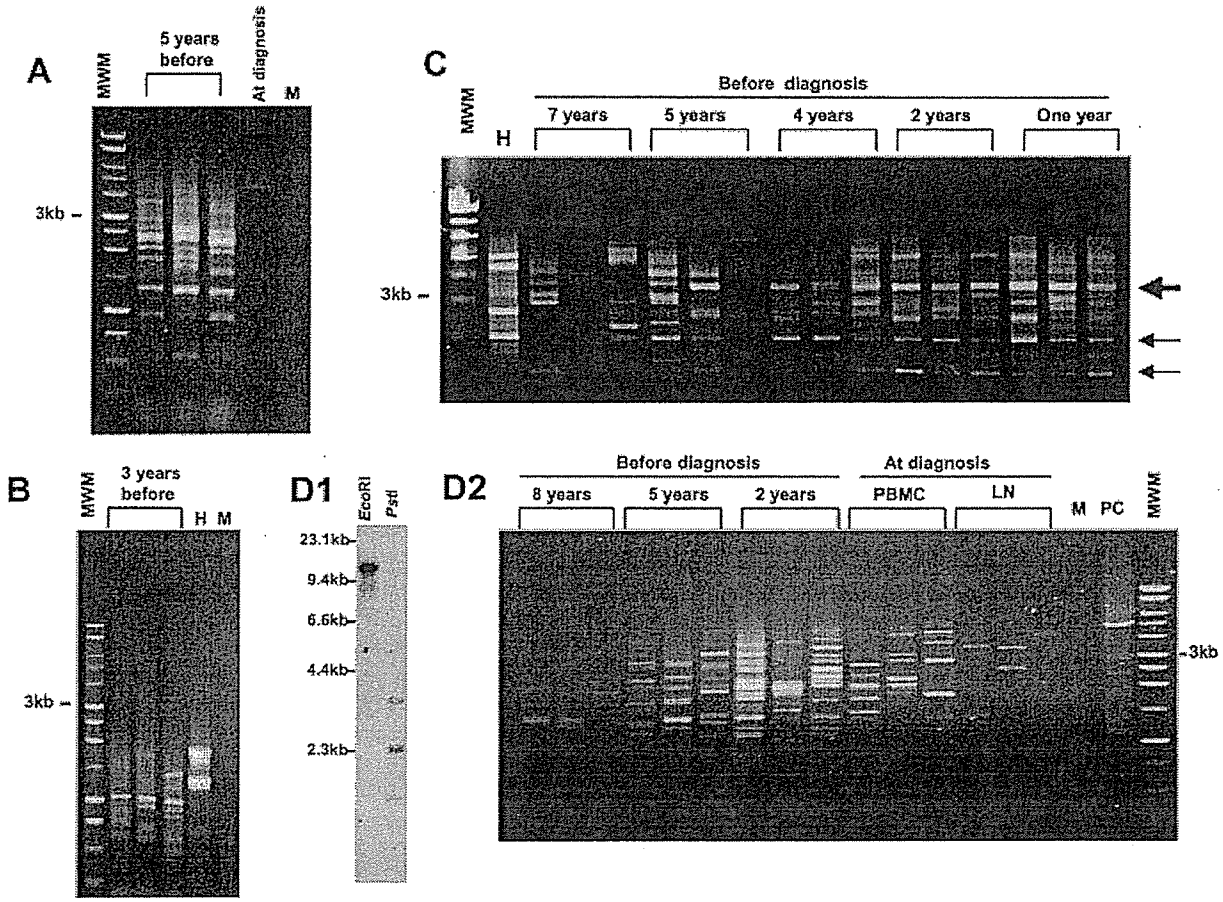

FIGURE 1 – Inverse-long PCR analysis of HTLV-1-infected cells in 4 cases before and at diagnosis of ATL. *(a)* Case 1. Triplicate analysis of PBMCs in the sample obtained 5 years before the onset of ATL and single analysis of ATL cells at diagnosis. *(b)* Case 2. Triplicate analysis of PBMCs in the sample obtained 3 years before the onset of ATL. *(c)* Case 3. Triplicate analysis of PBMCs in samples obtained 1–7 years before the onset of ATL. Arrows indicate major clones. *(d1)* Case 4. Southern blot analysis of lymph node biopsy specimen at diagnosis. EcoRI, EcoRI digestion; PstI, PstI digestion. *(d2)* Case 4. Triplicate inverse-long PCR analysis of PBMCs in samples obtained 2–8 years before the onset of ATL and from PBMC and lymph node (LN) samples obtained at diagnosis. MWM, m.w. marker (1 kb ladder); H, HUT102 cells as HTLV-1-positive control; M, Molt4 cells as HTLV-1-negative control; PC, leukemic cells obtained from an ATL patient, who was not a member of the study cohort, as a control.

load of the 37 age- and sex-matched HTLV-1$^+$ control subjects was 820 (10–9,790), which was significantly lower than the earliest prediagnostic proviral load of cases (Wilcoxon rank sum test, $p = 0.03$). In conditional logistic regression analysis, which accounted for the matched design (LogXact 4.1; Cytel, Cambridge, MA), there was a significant association between higher viral load and case status; the odds ratio of being an ATL case associated with each 1,000 copies (per 100,000 PBMCs) increase in viral load was 1.42 (95% exact confidence interval 1.04–2.10, $p = 0.03$).

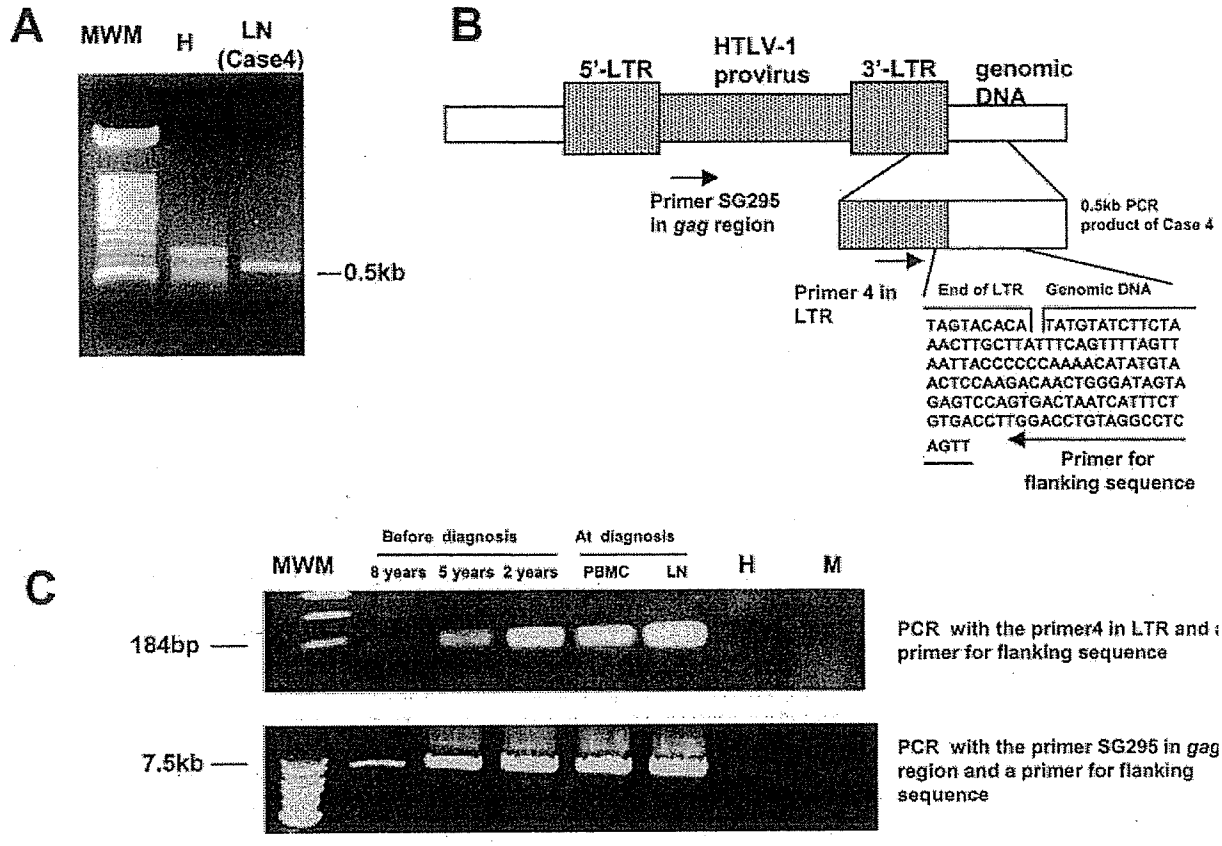

FIGURE 2 – Detection of the preleukemic clone in PBMC samples obtained from case 4 before diagnosis of ATL. *(a)* Inverse PCR analysis of lymph node (LN) specimen obtained at ATL diagnosis. *(b)* Schema showing subcloned and sequenced DNA of the inverse PCR amplicon derived from case 4 and the locations of primers used for leukemic clone-specific PCR. *(c)* Leukemic clone-specific PCR analysis using primer 4 of the LTR (upper panel) and primer SG295 (lower panel) before and at diagnosis of ATL. MWM, m.w. marker; H, HUT102 cells as HTLV-1-positive control; M, Molt4 cells as HTLV-1-negative control.

Although the number of cases analyzed was small, the difference in proviral load between cases and controls was striking and statistically significant. Our prospective analysis, thus, demonstrates an association between higher proviral DNA load and the subsequent development of ATL. HTLV-1 proviral DNA levels were stable over several years in asymptomatic carriers.[5] In cases 3 and 4, who had PBMC samples from more than 5 years, proviral levels were increased in samples obtained closest to the time of ATL diagnosis (1 and 2 years before onset, respectively). These increased proviral loads may reflect the clonal expansion of certain HTLV-1-infected cells.

Because the primers of the *pol* region were used for the quantitative assay of proviral DNA load, HTLV-1-infected cells with *pol*-defective provirus could not be detected by the current method. It is possible that the HTLV-1-infected cells with such defective virus were seen more commonly in carriers who developed ATL rather than in the control group because the defective provirus is sometimes found in patients with ATL.[16] As a result, the difference in proviral DNA load between cases and controls might have been larger if we had used a more conserved region, such as *tax*, for the primers.

We also examined whether the preleukemic HTLV-1-infected clone can be found prior to diagnosis in the peripheral blood of carriers who go on to develop ATL. To amplify the genomic DNA adjacent to the integration sites of the HTLV-1 provirus, inverse long-PCR was used.[12] All 4 cases had clonal bands of various sizes and intensities, indicating oligoclonal or polyclonal expansion of HTLV-1-harboring cells prior to diagnosis (Fig. 1). For case 1, a single band indicating the leukemic clone was detected in the peripheral blood by inverse long-PCR at diagnosis (Fig. 1*a*). Case 3, a carrier who developed lymphoma-type ATL, had several bands that were consistently strong over several years (arrows in Fig. 1*c*). These bands appear to represent major clones, consisting of large numbers of HTLV-1-infected cells with the same proviral integration site. One of the bands increased in intensity in the samples obtained close to the onset of ATL (large arrow in Fig. 1*c*). However, it was not possible to determine whether this clone was the preleukemic one because a sample from the time of ATL diagnosis for this carrier was not available.

For case 4, monoclonal integration of the HTLV-1 provirus in the leukemic cells from the lymph node was demonstrated by Southern blot assay at diagnosis (Fig.1*d1*). However, the